

**KARADENİZ TECHNICAL UNIVERSITY
THE GRADUATE SCHOOL OF NATURAL AND APPLIED SCIENCES**

DEPARTMENT OF ELECTRICAL AND ELECTRONICS ENGINEERING

**TRANSFORMERLESS PHOTOVOLTAIC SYSTEM FED SINGLE PHASE INDUCTION MOTOR
DRIVER FOR WATER PUMPING**

MASTERS OF SCIENCE THESIS

Syed Faizan Ali BUKHARI

**FEBRUARY 2020
TRABZON**



KARADENİZ TECHNICAL UNIVERSITY
THE GRADUATE SCHOOL OF NATURAL AND APPLIED SCIENCES
DEPARTMENT OF ELECTRICAL AND ELECTRONICS ENGINEERING

**TRANSFORMERLESS PHOTOVOLTAIC SYSTEM FED SINGLE PHASE INDUCTION
MOTOR DRIVER FOR WATER PUMPING**

Syed Faizan Ali BUKHARI

**This thesis is accepted to give the degree of
"MASTER OF SCIENCE"**

**By
The Graduate School of Natural and Applied Sciences at
Karadeniz Technical University**

The Date of Submission : 24 / 09 / 2019

The Date of Examination : 11 / 02 / 2020

Supervisor : Assist. Prof. Dr. Hakan KAHVECİ
Co-supervisor Assist. Prof. Dr. Mustafa Ergin ŞAHİN

Trabzon 2020

KARADENİZ TECHNICAL UNIVERSITY
THE GRADUATE SCHOOL OF NATURAL AND APPLIED SCIENCES

DEPARTMENT OF ELECTRICAL AND ELECTRONIS ENGINEERING
Syed Faizan Ali BUKHARI

**TRANSFORMERLESS PHOTOVOLTAIC SYSTEM FED SINGLE PHASE INDUCTION
MOTOR DRIVER FOR WATER PUMPING**

Has been accepted as a thesis of

MASTER OF SCIENCE

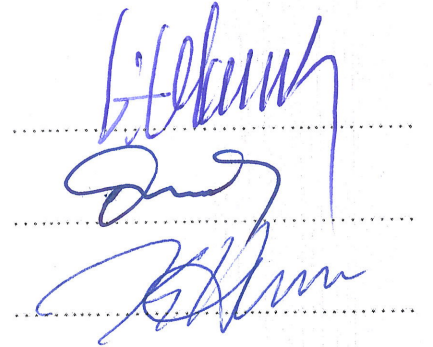
after the Examination by the Jury Assigned by the Administrative Board of
the Graduate School of Natural and Applied Sciences with the Decision Number 1820 dated
24 / 09 / 2019

Approved By

Chairman : Prof. Dr. Halil İbrahim OKUMUŞ

Member : Assoc. Prof. Dr. Mustafa AKTAŞ

Member : Assist. Prof. Dr. Hakan KAHVECİ



Prof. Dr. Asim KADIOĞLU
Director of Graduate School

ACKNOWLEDGMENT

I would like to pay my deep Gratitude and to express my thankfulness to my Supervisor Assistant Prof. Dr. Hakan KAHVECİ and Assistant Prof. Dr. Mustafa Ergin ŞAHİN who's expertise, knowledge and Friendly nature lead me to complete my work. Without his assistance it wouldn't have been so easy for me to fulfill my task.

Also, I would like to thank my family, especially my parents whose prayers and hard work made it possible to complete my masters today.

Lastly, I would also like to say thanks to Turkish Government and Türkiye Burslari scholarship program for providing me the opportunity to study in Karadeniz technical university for my master's degree.

Syed Faizan Ali BUKHARI

TRABZON 2020

THESIS STATEMENT

I hereby declare that all the information contained in this Master thesis entitled “Transformerless Photovoltaic System Fed Single Phase Induction Motor Driver for Water Pumping” completed under the supervision of Assistant Professor Dr. Hakan KAHVECİ and Assistant Professor Dr. Mustafa Ergin ŞAHİN. The presented work in this dissertation has not been submitted in any other university/institute for the award of any degree.
11/02/2020



Syed Faizan Ali BUKHARI

TABLE OF CONTENTS

	<u>Page</u>
ACKNOWLEDGMENT	III
THESIS STATEMENT	IV
TABLE OF CONTENTS	V
ÖZET	VIII
SUMMARY	IX
LIST OF FIGURES	X
NOTATIONS	XII
1. GENERAL INFORMATION	1
1.1. Introduction	1
1.2. Literature Review	4
1.3. Purpose of Study	5
1.4. Photo Voltaic Array	6
1.4.1. Efficiency of PV Cell	11
1.5. Boost Converter	12
1.6. Bidirectional Buck-Boost Converter	15
1.6.1. Boost Mode	17
1.6.1.1. Closed Switch S1	17
1.6.1.2. Open Switch S1	18
1.6.2. Component Design of the Converter	20
1.6.2.1. The Capacitance Design.....	20
1.6.2.2. The Inductance Design	20
1.6.3. Buck Mode	21
1.6.3.1. Closed Switch S2	21
1.6.3.2. Open Switch S2	22
1.6.4. Component Designs of the Converter are Operated Under Buck Mode	24
1.6.4.1. Inductance Design	25
1.7. PI Controller	26
1.8. Maximum Power Point Tracking – MPPT	28
1.8.1. Perturb and Observe	30

1.9.	Inverter Technology	31
1.9.1.	A Full-Bridge Inverter	31
1.9.2.	Pulse Width Modulation	32
1.9.3.	Unipolar Inverter	34
1.10.	V/F Control Based Scalar Control	34
1.11.	Single Phase Induction Motor	36
2.	CASE STUDY AND METHODOLOGY	41
2.1.	PV Array Design	41
2.2.	Design of DC-DC Converter	42
2.3.	MPPT Design	43
2.4.	Design of Buck-Boost Converter	44
2.5.	Single Phase Inverter Design	45
2.6.	Design of V/F Based Scalar Controller	46
2.7.	Main Topology Circuit Design With Controller	48
2.8.	Main Topology Circuit Design Without Controller	49
3.	RESULTS	51
3.1.	Simulation Results of PV array.....	51
3.1.1.	Voltage output of DC Bus Without Speed Control of Motor.....	51
3.1.2.	The Voltage output of DC Bus With Speed Control of Motor.....	52
3.2.	Simulation Results of Inverter Output Voltage	53
3.2.1.	Simulation Result of Sinusoidal Output Waveform	53
3.3.	Power Output Result of PV Array	54
3.3.1.	Output Waveform of PV Current and Voltage	54
3.3.2.	Simulation Results of PV Array With Change in Irradiance.....	55
3.3.3.	Simulation Result of PV Output Voltage and Current.....	55
3.4.	Simulation Results of Battery Output With Change in Motor Speed.....	56
3.4.1.	Simulation Results of Battery Output With Change in Irradiation	57
3.5.	Simulation Results of SPIM at Variable Speed Input	59
3.6.	Simulation Results of SPIM at Variable Irradiance Input	60
3.7.	Simulation Result of Speed Output of SPIM Without Controller	61
3.8.	Motor Main Winding Current Output.....	61
4.	DISCUSSION	62
5.	CONCLUSION AND FUTURE SCOPE	64

6. REFERENCES..... 65
CURRICULUM VITAE



Yüksek Lisans Tezi

ÖZET

TARIMSAL SULAMA İÇİN TRANSFORMATÖRSÜZ FOTOVOLTAİK SİSTEMDEN
BESLENEN TEK FAZLI İNDÜKSİYON MOTOR SÜRÜCÜSÜ

Syed Faizan Ali BUKHARI

Karadeniz Teknik Üniversitesi
Fen Bilimleri Enstitüsü
Elektrik-Elektronik Mühendisliği
Danışman: Dr. Öğr. Üyesi Hakan KAHVECİ
Eş-danışman: Dr. Öğr. Üyesi Mustafa Ergin ŞAHİN
2020, 69 Sayfa

Son zamanlarda kullanılan bağımsız bir sisteme örnek olarak, PV enerjisinin, nehirden suyu çoğunlukla kurak bölgedeki tarlalara pompalamak için sulama sürecinde kullanılmasıdır. Yağmur düşüşünün çok daha az olduğu yerlerde, şebekeye bağlı elektrik tedariki yetersizdir ve mahsul için sulama gereklidir. Artan petrol fiyatları nedeniyle, küresel ısınma ve fosil yakıtların sınırlı kaynakları, aynı tesise sınırlı kaynaklar sağlayarak ve daha iyi sonuçlar sağlayarak bunların hepsini en aza indirecek olan ikame ihtiyacını artırdı. Bu çalışma, santrifüjlü su pompasını çalıştırmak için tek fazlı bir endüksiyon motorunu besleyen tek fazlı transformatörsüz fotovoltaik sistemin tasarımını ve uygulanmasını ve en iyi performansı elde etmek için kullanılan metodolojiyi içerir. DC-DC Yükseltici dönüştürücü, PV dizisi üzerinden maksimum gücü çıkarmak için MPPT ve Buck-Boost kontrolör kullanılarak yapılan çıkış gerilimini en üst düzeye çıkarmak için kullanılır. DC gerilimi daha sonra AC çıkışını tek fazlı IMD'ye veren tek fazlı invertör kullanılarak AC çıkışına dönüştürülür. Tüm sonuçlar ve simülasyonlar Matlab simulink'inde yapılır.

Anahtar Kelimele: Maksimum güç noktası takibi, Asenkron motor, İntvertör, Güneş enerjisi sistem.

Master Thesis

SUMMARY

TRANSFORMERLESS PHOTOVOLTAIC SYSTEM FED SINGLE PHASE INDUCTION
MOTOR DRIVER FOR WATER PUMPING

Syed Faizan Ali BUKHARI

Karadeniz Technical University
The Graduate School of Natural and Applied Sciences
Department of Electrical-Electronics Engineering
Supervisor: Assist. Prof. Dr. Hakan KAHVECİ
Co-supervisor: Assist. Prof. Dr. Mustafa Ergin ŞAHİN
2020, 69 Pages

An example of the standalone system is that Photovoltaic energy is being used in irrigation process for pumping water from the river to fields mostly in arid region. Where rain fall is very less, supply of grid connected electricity is insufficient and watering is necessary for crop. To fulfil this blank there was a need of convenient and cheap technology which can help to overcome this issue. Due to rising oil prices, global warming and limited resources of fossil fuels have increased the need for substitution. This work includes the study of design and implementation of single phase transformerless photovoltaic system feeding a single-phase induction motor to run the centrifugal water pump and the methodology to achieve the best performance. DC-DC Boost converter is used to maximize the output voltage which was done by using MPPT and buck-boost controller by extracting the maximum power through the PV array. The DC voltage is then converter to AC output by using single phase inverter which gives the AC output to the single phase IMD. The system uses scalar control of motor in order to get the maximum output speed of the motor to run the centrifugal water pump. Computer simulations were practiced, and results are taken. All results and simulations are carried out in MATLAB Simulink.

Key Words: Maximum power point tracking, Induction motor, Inverter, Solar power system.

LIST OF FIGURES

	<u>Page</u>
Figure 1. A typical solar powered water pump system	4
Figure 2. Current voltage characteristic of PV array	7
Figure 3. Photovoltaic Array Electrical Equivalent Circuit.....	9
Figure 4. Boost converter	12
Figure 5. Circuit operation mode M1 and M2.....	13
Figure 6. Waveforms of the boost converter	14
Figure 7. Buck-boost converter	15
Figure 8. Charging of the converter while buck mode operating	16
Figure 9. Discharging of the converter while boost mode operating	16
Figure 10. The equivalent circuit with the closed switch S1 on the low-voltage side and the bi-directional buck-boost converter operating under boost mode.....	18
Figure 11. Boost mode of the buck-boost converter switch S1 is on the low-voltage	19
Figure 12. Buck mode of the converter when S2 is CLOSED on high voltage	22
Figure 13. Buck mode of the converter when S2 is open on high voltage	23
Figure 14. Waveforms of bidirectional buck-boost converter while buck mode	24
Figure 15. PI controller block diagram	27
Figure 16. SPV Array P-V and I-V Curve	29
Figure 17. Flow Chart - INC MPPT Algorithm	29
Figure 18. Flow chart Perturb Observe Algorithm	30
Figure 19. Full Bridge Inverter Circuit	31
Figure 20. PWM signal with different Duty cycle of modulated signal	32
Figure 21. Single phase H-Bridge Inverter	33
Figure 22. Waveforms of Unipolar Modulation Scheme	34
Figure 23. Single-Phase Induction Motor – Torque-Slip Characteristics	37
Figure 24. Single Phase Induction Motor Equivalent Circuit	38
Figure 25. Circuit Diagram of Capacitor Start Induction	39
Figure 26. Power and Current output of PV	41
Figure 27. Boost converter circuit diagram	42
Figure 28. MPPT controller.....	43
Figure 29. Buck-Boost converter	44

Figure 30.	VSI Circuit diagram	45
Figure 31.	Closed loop PI controller.....	46
Figure 32.	Voltage and frequency relation for the motor speed control.....	47
Figure 33.	Buck-Boost converter fed controlled water pumping system circuit design	48
Figure 34.	Buck-Boost converter fed controlled water pumping system circuit design without controller.....	49
Figure 35.	DC Bus Voltage output.	51
Figure 36.	Voltage output of Boost converter Time (secs)	52
Figure 37.	Inverter voltage across both legs	53
Figure 38.	Sinusoidal voltage output	53
Figure 39.	Time (secs) Power output PV array	54
Figure 40.	PV Current and Voltage Waveform.....	54
Figure 41.	PV Power output	55
Figure 42.	PV Current and Voltage Waveform.....	55
Figure 43.	Battery output (a) Charging and discharging mode (b)battery voltage (c) Battery current (d)battery voltage	56
Figure 44.	Battery output(a) Charging and discharging mode (b) Battery voltage c) Battery current (d) Battery voltage.....	57
Figure 45.	Times (secs) SPIM simulation output	59
Figure 46.	Time (secs) Figure 46. SPIM simulation output	60
Figure 47.	Speed output without controller at 1460rpm Time (secs) speed (rpm).....	61
Figure 48.	Main winding current (I) Time (secs)	61

NOTATIONS

AC	: Alternating Current
BLDC	: Brushless DC Electric Motor
DC	: Direct Current
SPIS	: Solar Panel Irrigation System
FF	: Fill Factor
IGBT	: Insulated-Gate Bipolar Transistor
IM	: Induction Motor
IMD	: Induction Motor Drive
MOSFET	: Metal Oxide Semiconductor Field-Effect Transistor
MPP	: Maximum Power Point
MPPT	: Maximum Power Point Tracking
PV	: Photo Voltaic
SEPIC	: Single-Ended Primary-Inductor Converter
SMPS	: Switched-Mode Power Supply
SPV	: Solar Photo Voltaic
SPWM	: Sinusoidal Pulse Width Modulation
SRM	: Slip Ring Machine
SVPWM	: Space Vector Pulse Width Modulation
THD	: Total Harmonic Distortion
V/F	: Voltage/Frequency
VSI	: Voltage Source Inverter

1. GENERAL INFORMATION

1.1. Introduction

The renewable sources of energy that are used for generating energy more specifically electricity, is solar, hydro, wind, ocean thermal, tidal, etc. that can be used for the energy conversion. As of March 31, 2017, the scenario of electricity production in India through renewable energy is about 57GWH that included solar, wind and biofuel as the sources of energy. India is also focusing to produce 175GWH energy from renewable energy sources including 100GW grid interacted solar electricity production in the coming time and hopefully before 2022. The solar energy is most economical, efficient and easily traceable as compared to all other sources of renewable energy that we know of, in terms of the cost and performance. As its not toxic, doesn't emit greenhouse gases, doesn't consume any fuel, has no maintenance cost and no water wastage obliges us to accept and say that photovoltaic (PV) array system provides clean and green energy with uninterrupted supply all through the day whenever solar irradiance available and even after that if it is stored through different ways.

Photovoltaic (PV) energy is widely used in homes, industries, remote areas, hospitals, in agriculture purposes, parks and public places etc. PV array is used as standalone and grid interacted system. In grid interacted system a large PV array plant is designed and power fed to grid which is used by the user. In standalone system PV array feeds power into specific equipment. Solar mobile chargers, solar lamps, solar fans etc. are best suitable example for standalone PV array system that we often easily find in households and in different places. The standalone PV system provides very good response and usage to the people in remote areas where grid power is unavailable or where continuous electricity supply is not available.

An example of the standalone system being used in recent time is that PV energy is being used in irrigation process for pumping water from the river to fields mostly in arid region. Where rain fall is very less, supply of grid connected electricity is insufficient and watering is necessary for crop, so it needs to get the water through any source possible.

Since around the year 2009 the price of solar panels started decreasing gradually, making this technology more affordable for agricultural process. Therefore, the process of

developing more powerful and efficient system got more attention in the international market which can withdrawal water from the greater depth. Prices continued to shake. By the year of 2025 the international renewable energy agency is trying to reduce the cost percentage of electricity generated by solar power PV by 59 percent as compare to the year 2015. Solar power irrigation system (SPIS) have enabled the development of low carbon irrigated agricultural system and provided the clean alternative to fossil fuels. In rural areas with very less electric facility this contributes the reliable electrification and reduce energy cost for irrigation. According to that, high-quality product and good service for small-scale farmers remains an issue in many countries. The development and design of the system must be user friendly and reliable so that a common worker can understand the basic of setup and can take care the daily operation and maintenance. In this whole report the importance of water resources assessment water consumption is also taken into account, SPIS can improve people's access to water by reducing the cost.

Solar technologies are becoming more suitable and feasible alternative for small and larger scale farmers due to the subsidy programs for solar powered irrigation systems as well as due to the reductions in the respective investment costs. The energy cost for irrigation is significantly reduced due to the affordable and reliable energy provided as the result of solar powered irrigation system. Both decentralized small-scale irrigation systems as well as the large-scale irrigation systems make use of the solar powered irrigation systems (SPIS). SPIS can provide alternative and relatively flexible energy source in the rural areas because there might be lack of reliable access to the electricity grid or diesel fuel might be expensive. It should be noted that without ample management and regulation, the SPIS can carry the risk of bolstering unsustainable water use. The significance of considering the risk stands despite the Life cycle assessments of SPIS that account for the emissions in a cradle-to-grave scenario. These assessments point towards possible decrease in the GHG emissions per unit of energy used for water pumping (CO₂-eq/kWh) of 97 to 98 % in comparison to the pumps working on diesel pumps (GIZ, 2016) and 95 to 97 % in comparison to grid electricity (global average energy mix). The installation of systems can lead to low field application efficiency, wasteful water usage and over-abstraction of ground water. This might occur because once the systems are installed, there can be lack of financial incentives for farmers to save on electricity or fuel for water pumping due to no cost per unit of power. In few situations, the overall water withdrawals are increased due to farmers selling water to their neighbors at a profit.

It should be observed that a lot of technical advances and innovations have been made, and various system configurations are now a possibility that were not considered before. As a result of reducing investment costs and increasing efficiency in the last years the SPIS sector has experienced fast variations. Therefore, there is no relevance in the reports originating from the past. The electronic/software features in general and Maximum Power Point Tracking (MPPT) specifically lead to improved efficiency during the cloud interfaces, solar day and variable motor speed.

Irrigation system (flood, sprinkler, micro-irrigation [drip] and irrigation machines are used for direct pumping PV panels and pump with DC or AC motor, controller with or without water storage (elevated) tank or reservoir. The electronic/software features in general and Maximum Power Point Tracking (MPPT) specifically lead to improved efficiency during the cloud interfaces, solar day and variable motor speed.

It is widely utilized system around the world; there are more than 50% water to wire efficiencies derived from efficient systems. There is a need for speed control for irrigation machines and the usage should be based on volume.

If solar energy is not required for alternative uses, then it can be utilized for income generation as well as for powering grid. Therefore, significant compromises on efficiency are necessary despite various uses being accounted for and paid for.

The solar pump systems operate simultaneously with the diesel/electrical grid pumps. For the high season (Demand for water) energy or normal nighttime usage blends at low radiation level. There is a reduction in peak demand for size of solar generator. Different configurations for manual and automatic systems exist that are often used with the already existing diesel pumps. For example; First configuration can be missing power from solar sources being supplemented according to the need and second configuration can be in case of solar sources not producing the required energy where system can switch to the external energy source.

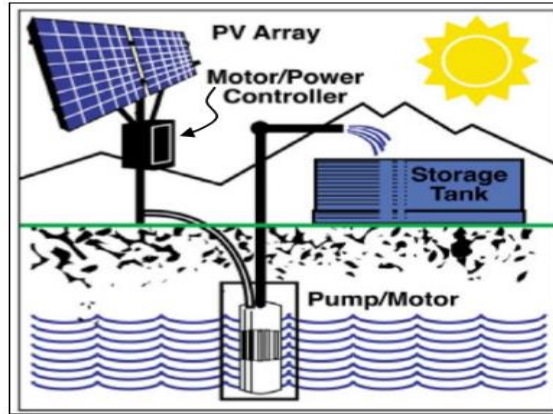


Figure 1. A typical solar powered water pump system.

Well sized solar pumps can support sprinkler, pivot, drip or food irrigation methods. A system can also include fertigation or filtration depending upon the local conditions. Low pressure drips are often attached with solar pumps. To fill the tank with water the required pressure is achieved and then water is released through gravity. However, the tank cost is sometime more than the pump which makes the system more expensive. The direct connection of the drip system to the pump causes problem due to the change in pressure and flow rate of the solar pump with varying insolation.

To maintain power output and pressure for long time solar trackers could be helpful, but they are more costly. Positioning of solar panel also plays very important role to maintain constant power and pressure, like splitting it between east and west directions will also achieve constant power/pressure for the irrigation system. In general, the cost of an elevated tank or tracking system will be more than the cost of additional panels.

It is important to consider trade-offs between oversized pumping system and storage tank. The reason is that irrigation is carried out on daily basis, according on the climate conditions as well as the crop and soil kinds.

1.2. Literature Review

In reference [1], independently two single phase induction machines with different speed fed by 3-Phase VSI (Voltage Source Inverter) is implemented. A closed loop space vector pulse width modulation (SVPWM) based V/F scalar control is employed.

In reference [2-6], SPV fed induction motor drive (IMD) for water pumping system is applied. In reference [2-3] vector controlled IMD implemented. To increase the efficiency

and decrease losses a minimization technique is proposed. In reference [4], sensor less vector control of IMD is implemented. The defined system works in two platforms which includes direct conversion of DC-AC from PV without DC-DC converter.

In reference [5], V/F control of IM water pumping system is applied. The INC MPPT algorithm is implemented for controlling DC-DC boost converter and V/F based SPWM is used for controlling VSI. In reference [6], direct torque control of IMD is implemented.

In reference [7], the past decades a large number of researchers have given the theory about the standalone PV systems which were used to operate three phase induction motor as well as single phase induction motor for the low voltage operations for example modeling and simulation of the bidirectional buck boost converter for the electrical vehicle applications. In which permanent magnetic induction motor was operated with the help of DC-DC converter as well as three phase inverters in order to control the motor speed as well as charging and discharging of the battery for the required back up.

The literature survey reveals that most of the researchers have carried out their work in the field of water pumping was mostly related to three phase machines like IMD, BLDC etc.

Perturb and observe method is simple to implement as compare to other methods. In this method PV array is perturbed in the direction of irradiation. The operating point reaches the MPP when the power extraction is increased, and the voltage continue to perturb in the same direction. The operating points move away from the MPP when the power extraction is decreased so the direction of voltage perturbation is needed to be changed. The oscillation at the steady state is the main drawback of this method. Liu et al. [31]. has tried to solve this problem in their study. The output power change is calculated in this method. If the change is negative the operating voltage would be decreased, if the change is positive the operating voltage would be increased. Carolin Mabel and Suganya [32] have improvised the perturb and observation method which operates at desired performance at unchanged irradiation conditions.

1.3. Purpose of Study

Water sources are very important for agriculture. Water should be effectively used in the agricultural sectors. Otherwise, these water resources will be used ineffectively and will run out sooner overtime. In precise farming applications, the amount of water needed by the

crop needs to be transmitted to the soil in some way. Otherwise, the yield of the product will decrease.

In some countries, especially in Africa, the energy of the pumps used in irrigation of agricultural areas is supplied from the plant, diesel generators or hybrid from these two. The demand of irrigation system is getting higher with time due to the increase in population. The population increment causes the high food consumption which needs the better and more crop production, but the continuous climate change causes the problem in crop production. High electricity and diesel costs are affecting the pumping process for the irrigation for farmers. There are many rural areas which don't have grid electricity or few of them having continuously load shedding issues. In recent years, solar water pumping systems have become popular, especially with the decrease in PV panel costs.

In this study, "solar irrigation system", which will be the basis for precise agricultural practices, has been proposed. The amount of water to be pumped according to the soil moisture condition can be adjusted with this system. The system will be independent from the grid. It is in hybrid structure consisting of PV panels and battery group. However, moisture sensing and pump speed determination are not included in the thesis.

In the proposed hybrid system, the water pump was driven by a "single phase induction motor". Motor speed control was done with (v / f) closed loop scalar control. The unipolar sine pulse width modulation (SPWM) technique has been used for the single-phase inverter and, bidirectional DC-DC converter has been used to charge or discharge the battery group.

The proposed system storage can be used for irrigation systems with the tank or drip irrigation systems.

1.4. Photovoltaic Array

Due to the distributed generation, fossil fuel depletion, and increasing electricity demands, the PV (photovoltaic) power generation system has emerged as one of the most promising sources of renewable energy [1]. In accordance with the study of [2], one of the biggest problems that are threatening the power sector includes increasing demands of electricity and unavailability of the viable sources. This situation has resulted in increasing the demands of renewable energy sources, like solar and wind energy. It is since the continued utilization of fossil fuels has not only exerted burden on the economy, but it has

also been the prime reason behind the depletion of the biosphere and rising global warming. In this account [3] has contended that the popularity of renewable energy sources has greatly been increased in the past few years due to rising environmental concerns, increasing energy prices, and elevating energy demands. In this account, several renewable energy sources are available, like wind, marine, etc. However, PV is amid one of the most reliable and up-to-dated sources that are successfully addressing high energy demands.

As far as the discovery of PV cells is concerned, its history dates to the era of the early 1880s. Afterwards, during the era of 1950s silicon-based cell was developed at the bell laboratory. Later, during the period of the 1980s a more advanced and state-of-the-art solar photovoltaic energy was invented that gained immense popularity during 1990s. Since that time, numerous researches are being carried out for the sake of developing such a PV cell that is of high efficiency and minimum cost. Though PV cell various benefits, in terms of lower emissions, but its initial installation cost is too high, and it offers the efficiency of five to six percent, which is the biggest concern for its users. If current trends are taken into consideration, consumer solar panel offers the efficiency of 15-16 per cent. On the other hand, 27 per cent of the efficiency is reported to be offered by the solar panels that are developed for commercial use. However, as per the opinion of the industry experts, the highly efficient solar photovoltaic system is the one that gives the efficiency of approximately 44.7 per cent. Therefore, it can be affirmed that the prominent concerns that are associated with the photovoltaic cells are related to intermittency, efficiency, as well as the initial installation cost.

Photovoltaic array is a combination of several cells arranged in series and parallel connection. The I-V characteristic is shown in Figure 2.

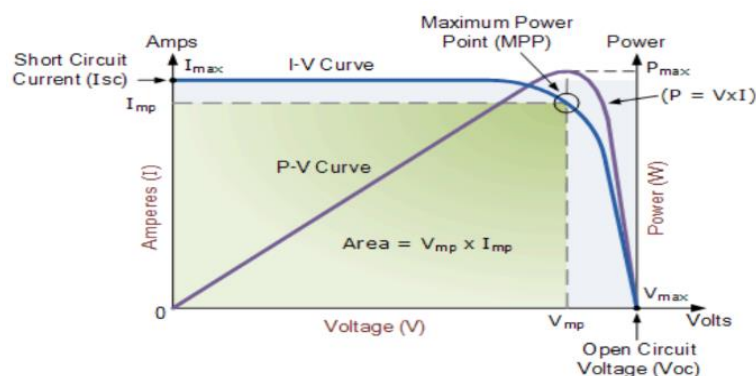


Figure 2. Current voltage characteristic of PV array [17]

Solar cells are connected in series and parallel to increase the power generation. When they are connected in parallel the current produced is increased and when they are connected in series the voltage produced is increased, anyhow by both ways the generated power is increased.

While highlighting the significance of solar energy [4] has proclaimed that solar radiations could be the greatest way of tackling with the energy crises. As per the author, in the past few years, the power conversion mechanisms have been significantly minimized in size. In addition to this, the recent advancements in the field of material science and power electronics have also facilitated the engineers to develop portable, but resilient systems to handle high power demands. However, there exists a drawback of these systems, i.e., high power density. In this regard, the multi-input converter units are widely been used to adequately handle voltage fluctuations. Still due to minimal efficiency of these systems and high cost of production they could not gain much attention in the power generation sector. It is anticipated that the continuous increment in the manufacturing of solar cell technology will make the widespread use of these systems possible.

It has been asserted that all the renewable energy sources, solar power systems have gained immense fame as they excellently generate a huge amount of electrical energy along with minimal greenhouse emissions [5]. In short, solar power systems have been regarded as the unique and most optimal solution to rising energy demands. However, as per the study of [6] though solar power systems possess immense benefits they are incapable of offering desirable efficiency. It is since the solar cell's efficiency is dependent on several factors that include shadow, dirt, spectral characteristics of sunlight, insolation, temperature, etc. Due to climatic variations, like increment in the ambient temperature and cloudy weather may result in changing panel's isolation; thereby, resulting in the minimization of the PV (photovoltaic) array output power. In other words, it can be proclaimed that each photovoltaic cell generates energy as per its environmental as well as operational conditions [7] [8].

As far as the working mechanism and functionality of PV cells are concerned, it is found that advanced technology can convert the sunlight (receiving from the sun) into DC power. Basically, the entire PV array is composed of several solar cells that have a parallel and series connection for getting the desirable current and voltage. The PV cell can be substituted by the equivalent electric circuit that is comprised of a diode, series resistant, shunt resistance, as well as a power supply mechanism (figure 3). When R – resistive load is connected to the PV cell then cell's working power will have a load as well as crossing

point v-amp characteristic. As mentioned earlier in this section, numerous environmental factors can impact the functionality of the solar photovoltaic array. Some of these factors include clouds, external temperature, the intensity of the solar beams, etc.

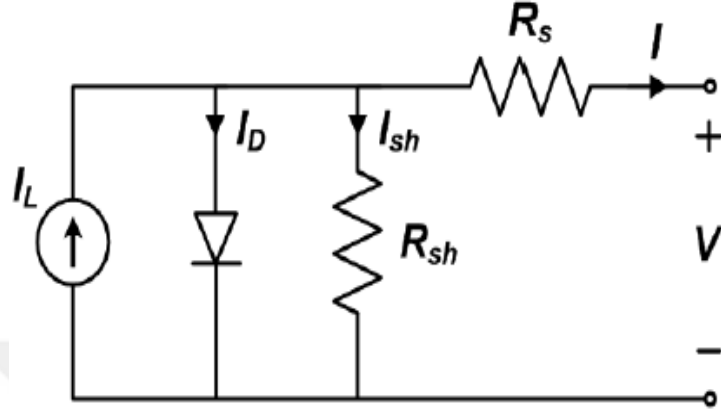


Figure 3. Photovoltaic array electrical equivalent circuit.

$$I_D = I_o \left[e^{\frac{V_c, q}{a \cdot k \cdot T_{ck}}} - 1 \right] \quad (1)$$

- " I_D " is dark current (A),
- " I_o " is saturation current of the diode (A),
- " V_c " is cell voltage (V),
- "q" is the charge of an electron,
- "a" is the diode ideality constant,
- "k" is the Boltzmann's constant
- " T_{ck} " is the cell temperature.

The relation between the net current I , light generated current I_L and the normal diode current I_D is defined by the equation (2).

$$I = I_L - I_D \quad (2)$$

In addition, equation (3) presents the simplified model as shown in Figure 3.

$$I = I_L - I_o \left[e^{\frac{(V+I \cdot R_s)}{a \cdot k \cdot T_{ck}}} - 1 \right] \quad (3)$$

So that equivalent circuit of an ideal solar cell can be represented as shown in Figure 2 with an ideal current source in anti-parallel with a diode.

In practice solar cells have some losses. These losses occur because of the resistance in series (R_s) and another in parallel (R_{sh}). The final model is as shown in Figure 2.

If we take account, these resistances equation (3) can be written as (4).

$$I = I_L - I_0 \left[e^{\frac{(V+I R_S)}{a.k.T_c K}} - 1 \right] - \frac{V+I R_S}{R_{sh}} \quad (4)$$

The photocurrent depends on the solar insolation and cell's working temperature, which is described as [21, 22]

$$I_L = [I_{SC} + K_1(T_C - T_{ref})] \frac{G}{G_{ref}} \quad (5)$$

Where I_{SC} = solar cell short-circuit's current, G_{ref} = reference solar insolation in W/m^2 , T_{ref} = cell's reference temperature, T_C = operating temperature, K_1 = cell's short-circuit current temperature coefficient, and G = solar insolation in W/m^2 . Another important characteristic of PV cell is Fill factor (FF). The value of FF is somewhere between 0.4 to 0.8 but the ideal photovoltaic system has the fill factor of 1.0.

$$FF = \frac{P_{max}}{V_{OC} \cdot I_{SC}} \quad (6)$$

Like other semiconductor devices, solar photovoltaic arrays are also temperature sensitive. It is mainly because the rising temperatures reduce the band gap energy that eventually results in effecting the open circuit voltage. Specifically, for the silicon-based components, this phenomenon results in the minimization of the voltage, i.e., up to 2.2 mV/degree centigrade. In case of varying V_{oc} , the overall power (at the output end), as well as other parameters, get changed.

Since the intensity of sunlight changes daily, the impact of R_{sh} (shunt resistance) at low sunlight intensity becomes extremely crucial. The decreasing irradiance bias point results in decreasing the current (passing through solar cell). Not only this, but it also leads to solar cell's equivalent resistance to the shunt resistant. Since both resistances are same, it

results in increasing the value of the current passing through the shunt resistance; hence, elevating the power loss, mainly because of the shunt resistance. Thereby, it can be contended that in the cloudy data, the photovoltaic cells hold a greater value of its original power as compared to the one that has a low R_{sh} . The research work of [9] also adheres to these findings and have inspected the performance, efficiency, as well as the development aspects of solar photovoltaic systems.

1.4.1. Efficiency of PV Cell

The efficiency of the PV cell means the performance output given by the PV array depending upon the conditions which affects its respective structure and design. It's measured with respect to all those necessary conditions which are affective over its performance. Higher the efficiency higher the performance we can get by any PV array which means the higher amount of sunlight converted to electricity. To determine the efficiency there are several methods used, one of the most common method used is Standard Test Condition (STC). The efficiency of the most of the available PV arrays in the market is in between %15 to 22 % determined over the STC rule with the temperature of 25 degree Celsius and $1000W/m^2$. There are three different types of the solar cells depending upon their efficiency.

They are as following,

- Monocrystalline cells
- Thin-film cells
- Polycrystalline cells

The efficiency of polycrystalline cells is between %14 to %16. The efficiency of the monocrystalline cells is between %20 to %22. The efficiency of thin-film cells is between %7 to %12.

Many amendments have been made in the year 2016 to improve the efficiency of the solar cells which gave the positive results with the increment of %6 to 18% in the performance. Recent researches have given the result of 44.7% efficiency of the pv cells which can be further improved by the percentage of 50% [7].

1.5. Boost Converter

The figure given below shows the boost converter which always gives the increased output for the given input voltage,

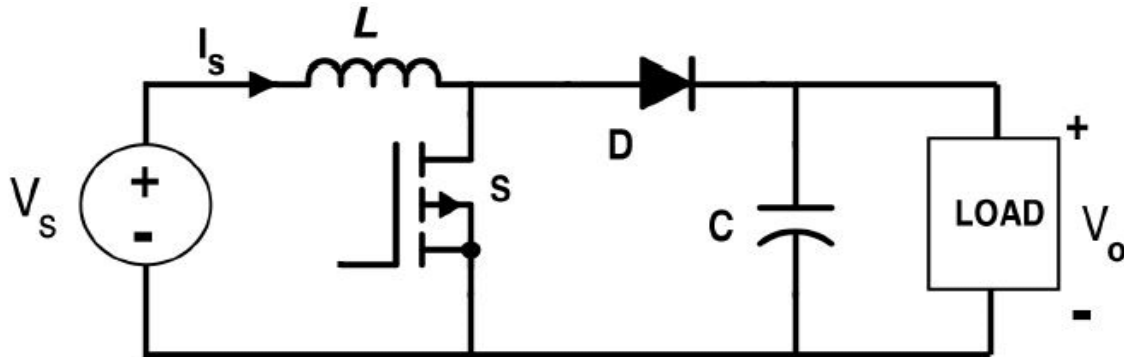


Figure 4. Boost converter.

In the figure 4 the block diagram of the boost converter is given depending upon the several electronics components to control the voltage output. The main component is MOSFET switch which is controlled by the gate signal. The gate signal is continuously switching MOSFET by means of duty cycle. The duty cycle determines the switching process of MOSFET for the voltage control purpose and to find the maximum power point of the photovoltaic array. In order to give the proper duty cycle MPPT system is used to find out the exact point where the system can operate. There are several MPPT methods for this, but the most commonly used method is Perturb and Observe method where system is continuously invigilated by mean of increment and the decrement of the duty value in order to locate the best operating point for MPPT process. The values of the electronic components like capacitor, inductor and the load resistor are given in the system design section.

There are two modes of operation for the boost converter as shown in the figure 5.

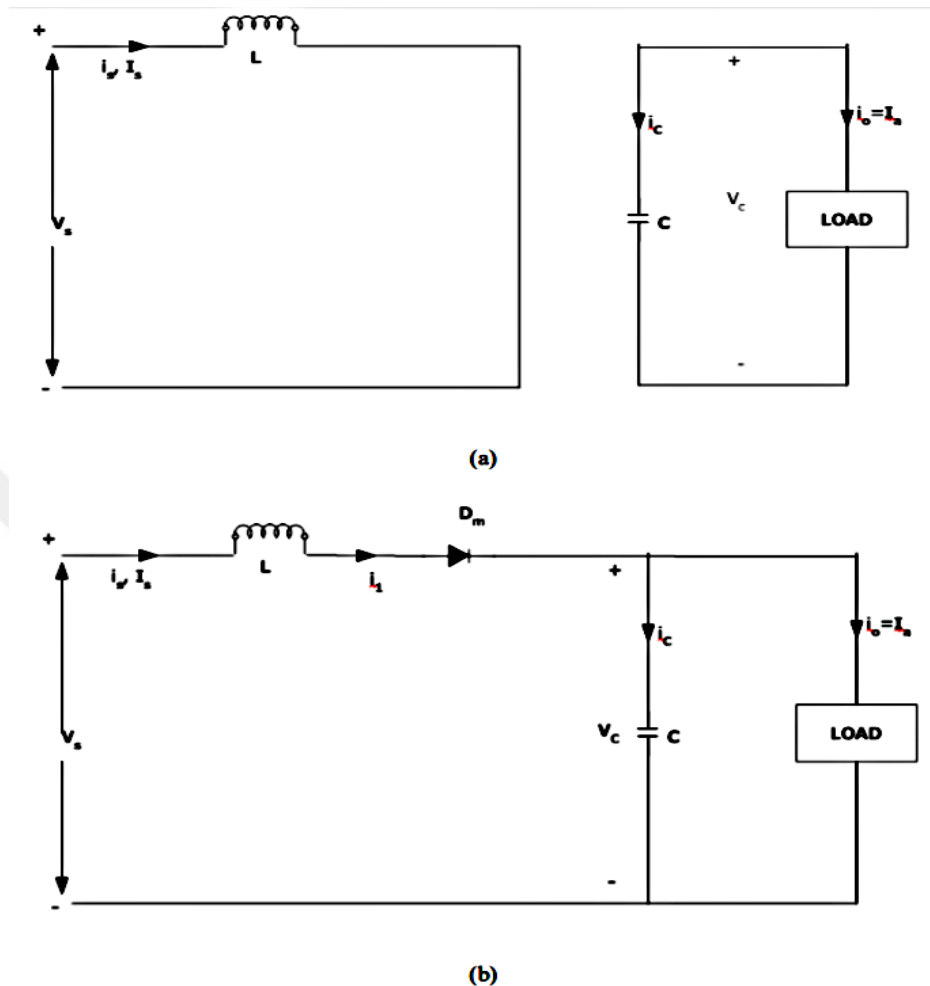


Figure 5. Circuit operation mode M1 and M2.

There are two operating functional modes of the boost converter, Mode1 and Mode2. At time=0 the mode M1 starts when the transistor is switched on. The input current increases and flows through the transistor and the inductor L. at the time $t=t_1$ the transistor is switched off and the input current flows through C, L, diode and load. The inductor current decreases until the next cycle starts. The stored energy in inductor flows through the load.

The waveform for the voltage and current is shown as following.

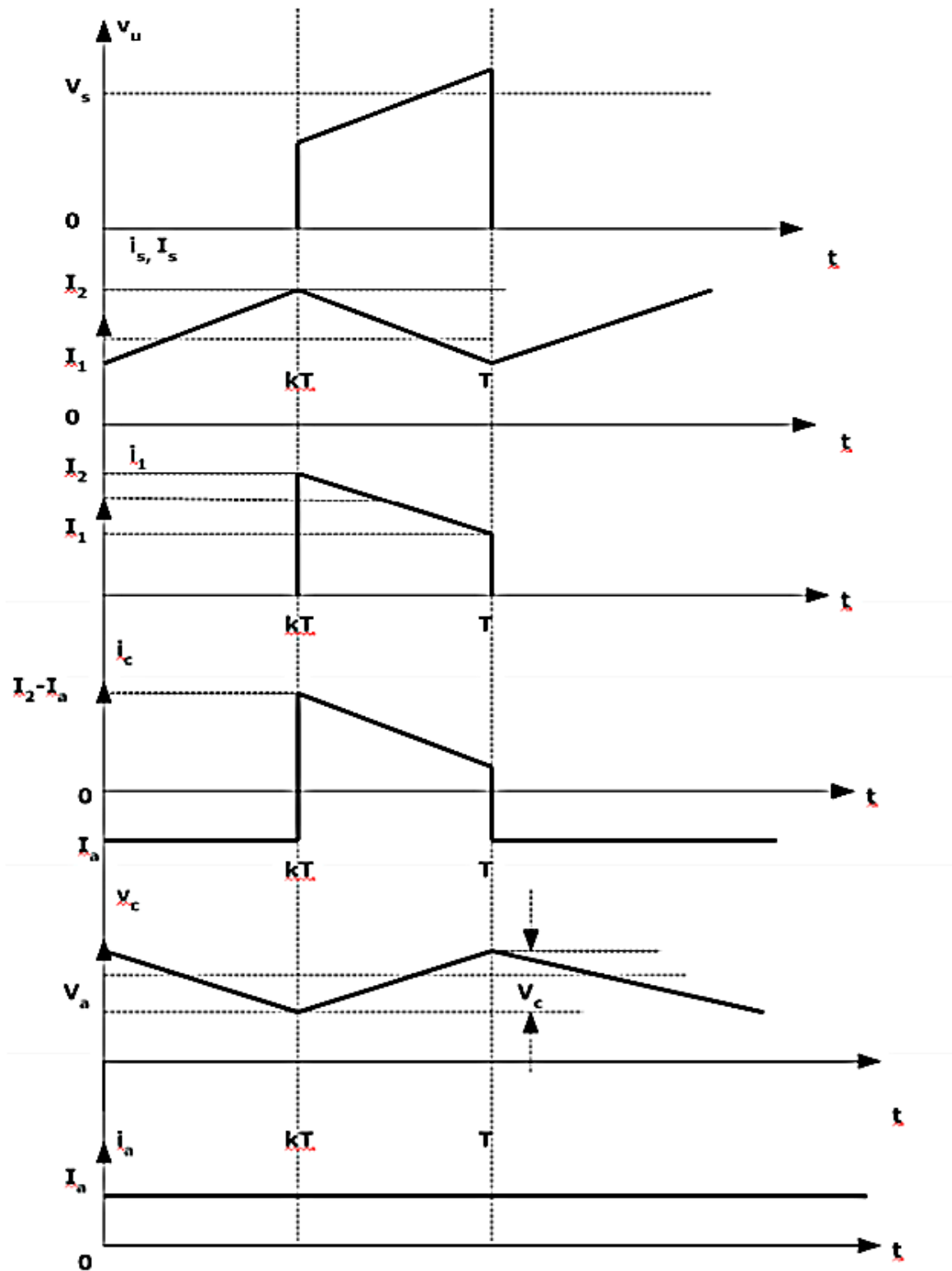


Figure 6. Switching waveforms of the boost converter [24].

While working switch 1 gives the output voltage equation as

$$V_O = \frac{V_{dc}}{1-D} \quad (7)$$

The ripple peak to peak current of the inductor is as follows

Output average voltage is given as follows

$$I_S = \frac{I_O}{1-D} \quad (9)$$

$$\Delta I_L = \frac{V_{DC}}{L} \times DT \quad (10)$$

$$\Delta V_O = \frac{I_O DT}{C} \quad (11)$$

ΔI_L is ripple current in inductor and ΔV_O ripple voltage in output DC voltage. ΔI_L and ΔV_O both is maximum at $D=1$ which is not preferable due to continuous charging of inductor.

This boost converter increases the output voltage at the specified level and MPPT controller helps to make the voltage constant at 325 volts which is enough to operate the motor.

1.6. Bidirectional Buck-Boost Converter

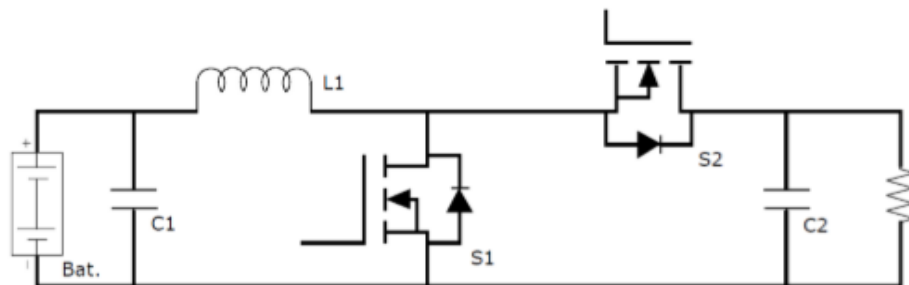


Figure 7. Buck-boost converter.

In the figure above a buck boost converter can be seen with MOSFET arrangement of left to right arranged switches according to the arranged pattern the boost converter can be

seen at left and at right it's the buck converter. by the usage of MOSFET we can reduce the amount of components in the converter to save cost as well as losses. The boost inductor plays the role for the filter here. MOSFET are capable to work with high switching frequency which reduces the size of filter and magnetic components. Performance is also better due to the antiparallel diodes attached with the switches which helps in the rectifying and freewheeling periods [10].

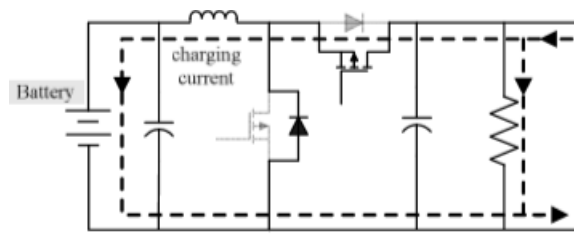


Figure 8. Charging of the converter while buck mode operating.

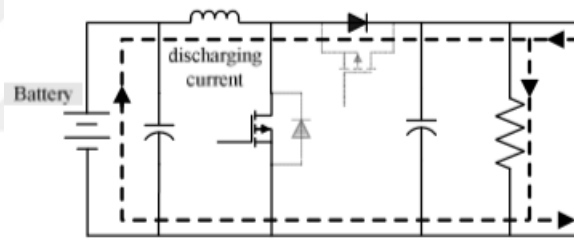


Figure 9. Discharging of the converter while boost mode operating.

The operating modes of the bidirectional dc converter is shown above in the figure 9. There are two operating modes the first one shows the charging and the second one shows the discharging mode of the DC-DC converters. if the energy supplied by the PV panel isn't sufficient for the load which is induction motor of 2000KW then it will work as a boost converter showed in figure b to maintain the output voltage at 325 or accordingly to supply the required power and voltage and the converter will start working as boost converter by using the left switch the battery will be discharged at the moment. Secondly if the voltage supplied by the PV panel is more than the required voltage and power the converter will start working as buck converter again to stabilize the voltage and the battery will be charged. The equation of the duty cycle of the converters is expressed as

$$D_{Boost} = 1 - \frac{V_{pv}}{V_{dc}} \quad (12)$$

$$D_{Buck} = \frac{V_{bat}}{V_{dc}} \quad (13)$$

Here boost is the duty cycle of the boost converter, buck is the duty cycle of the buck converter and V_{bat} is the battery voltage.

Connecting two switches in the series and the equation will be as following.

$$D = D_{Boost} \cdot D_{Buck} = \left(1 - \frac{V_G}{V_{dc}}\right) \left(\frac{V_{bat}}{V_{dc}}\right) = \frac{V_{bat}}{V_{dc}} - \frac{V_{bat}}{V_{dc}^2} V_G \quad (14)$$

1.6.1. Boost Mode

1.6.1.1. Closed Switch S1

Due to the complementary mechanism between the switches one is on the high and the other is on the low voltage so according to that here switch s1 is one the low voltage of the converter represents the closed side and the other switch s2 is on the high voltage of the converter represents the high voltage side. in the respective mode the inductor L_m and the low-voltage supply V_L are parallel which cause the both inductor and low voltage to be equal. The circuit voltage is written is as following.

$$V_{Lm} = V_L - V_H = L_M \frac{di_{Lm}}{dt} \quad (15)$$

When the switch is closed the rate of change of the inductor voltage L_m is constant therefore it represents a linear increase in inductor current expressed by the following equation.

$$\frac{\Delta i_{Lm}}{\Delta t} = \frac{\Delta i_{Lm}}{DT} = \frac{V_L}{L_m} \quad (16)$$

The following can be obtained:

$$\Delta i_{Lm(on)} = \frac{V_L}{L_m} DT \quad (17)$$

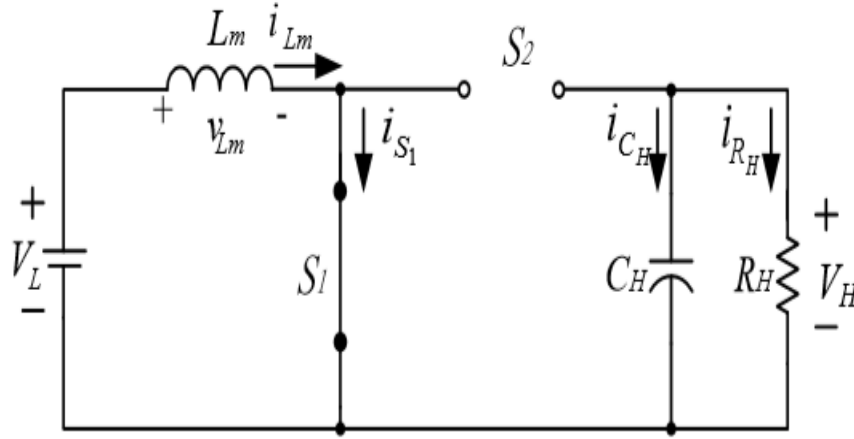


Figure 10. The equivalent circuit with the closed switch S1 on the low voltage side and the bi-directional buck-boost converter operating under boost mode.

1.6.1.2. Open Switch S1

When the S2 switch represents the high voltage side and closed state and S1 on the low voltage side represents open mode. The inductor voltage V_{Lm} can be expressed as [10].

$$V_{Lm} = V_L - V_H = L_m \frac{di_{Lm}}{dt} \quad (18)$$

Simplifying it

$$\frac{di_{Lm}}{dt} = \frac{V_L - V_H}{L_m} \quad (19)$$

There is a linear decrease in inductor voltage i_{Lm} when switch S1 is open. This can be express as

$$\frac{\Delta i_{Lm}}{\Delta t} = \frac{\Delta i_{Lm}}{(1-D)T} = \frac{V_L - V_H}{L_m} \quad (20)$$

From the above equation the following equation can be written as

$$\Delta i_{Lm(off)} = \frac{(V_L - V_H)}{L} (1 - D)T \quad (21)$$

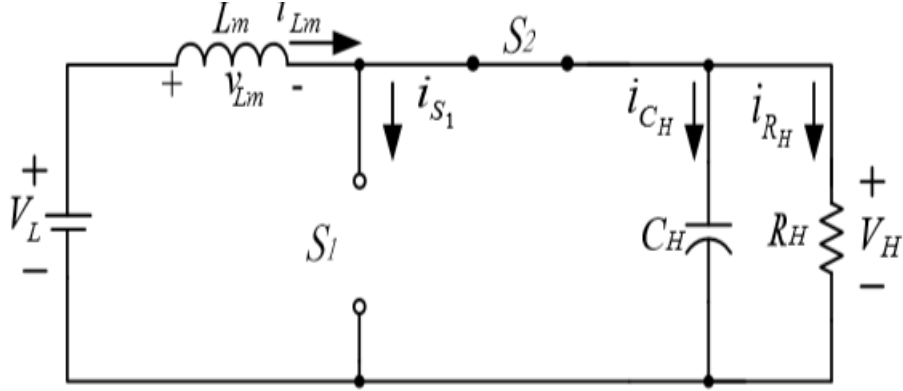


Figure 11. Boost mode of the buck-boost converter with the switch S_1 is on the low-voltage side.

The above figure shows the equivalent circuit. Under a steady-state operation, the change of the converter's inductor current i_{L_m} in a single cycle of operation must equal zero, that is.

$$\Delta i_{L_m(on)} + \Delta i_{L_m(off)} = 0 \quad (22)$$

By incorporating (17) and (21) into (22), the following can be obtained

$$\frac{V_L}{L_m} DT + \frac{(V_L - V_H)}{L_m} (1 - D)T = 0 \quad (23)$$

Simplifying 12

$$V_L DT + (V_L - V_H)(1 - D) = 0 \quad (24)$$

The relationship between the low and the high voltage side can be determined as

$$V_H = \frac{1}{1-D} V_L \quad (25)$$

This shows that the voltage V_H on the high-voltage side is greater as compared to the low voltage side V_L .

1.6.2. Component Design of the Converter

1.6.2.1. The Capacitance Design

According to the above analysis it is assumed that for the value of capacitor C_H is capable of maintain the voltage V_H on the high-voltage side of the converter. The variable charges on capacitor C_H are as follows

$$\Delta Q_H = \frac{V_H}{R_H} DT = C_H \Delta V_H \quad (26)$$

From (16), the ripple voltage can be expressed as

$$\Delta V_H = \frac{V_H DT}{R_H C_H} = \frac{V_H D}{R_H C_H f} \quad (27)$$

Simplifying (24),

$$C_H = \frac{C_H}{R_H f (\Delta V_H / V_H)} \quad (28)$$

Where f is the switching frequency and R_H is the equivalent load resistance on the high voltage side of the converter, and $\Delta V_H / V_H$ is the ripple ration of the voltage.

1.6.2.2. The Inductance Design

If we neglect the loss the input power P_L should be equal to the output power P_H of the converter, the following can be expressed:

$$V_L I_{Lm} = \frac{V_H^2}{R_H} = \frac{(V_L / (1-D))^2}{R_H} = \frac{V_L^2}{(1-D)^2 R_H} \quad (29)$$

So, we can get the mean value I_{Lm} of the inductor current as following:

$$I_{Lm} = \frac{V_L}{(1-D)^2 R_H} \quad (30)$$

The maximum and minimum values for the inductor current can be obtained through (17) and (30).

$$I_{Lm-max} = I_{Lm} + \frac{\Delta I_{Lm}}{2} = \frac{V_L}{(1-D)^2 R_H} + \frac{V_L}{2L_M} DT \quad (31)$$

$$I_{Lm-min} = I_{Lm} - \frac{\Delta I_{Lm}}{2} = \frac{V_L}{(1-D)^2 R_H} - \frac{V_L}{2L_M} DT \quad (32)$$

The minimum value of the inductor must be greater the zero in order to operate in the continuous conduction mode. Thus (32) must be satisfied

$$\frac{V_L}{(1-D)^2 R_H} - \frac{V_L}{2L_M} DT \geq 0 \quad (33)$$

To operate in CCM the minimum inductor current value must be satisfied

$$L_{m,min} \geq \frac{D(1-D)^2 R_H}{(1-D)^2 2f} \quad (34)$$

To operate in boost mode simultaneously the converter needs to operate in the CCM in any duty cycle. The value D of the duty cycle increased from 0 to 1.

1.6.3. Buck Mode

1.6.3.1. Closed Switch S2

When switch S2 is on the high and the switch S1 is on the low voltage side of the converter it presents an open state. The inductor voltage L_m on the both sides can be expressed as following:

$$V_{Lm} = V_H - V_L = L_m \frac{di_{Lm}}{dt} \quad (35)$$

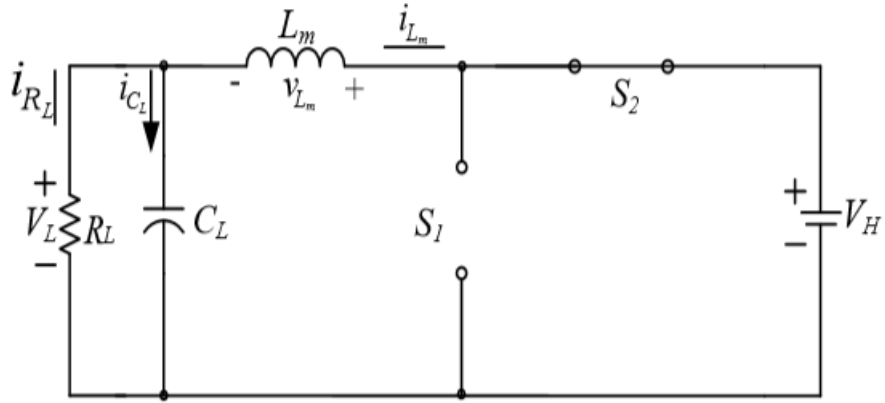


Figure 12. Buck mode of the converter when S2 is CLOSED on high voltage

Simplifying equation (35),

$$\frac{di_{Lm}}{dt} = \frac{(V_H - V_L)}{L_m} \quad (36)$$

While this mode there is a linear increment in the inductor current with the positive value. When the switch is closed the change of the inductor current can be observed as;

$$\frac{\Delta i_{Lm}}{\Delta t} = \frac{\Delta i_{Lm}}{DT} = \frac{(V_H - V_L)}{L_m} \quad (37)$$

From (37);

$$\Delta i_{Lm(on)} = \frac{(V_H - V_L)}{L_m} DT \quad (38)$$

1.6.3.2. Open Switch S2

When S2 is on high and S1 is on the low-voltage side it represents the closed state. The equivalent circuit is as following

$$V_{Lm} = -V_L = L_m \frac{di_{Lm}}{dt} \quad (39)$$

Simplifying equation (36);

$$\frac{di_{Lm}}{dt} = -\frac{V_L - V_H}{L_m} \quad (40)$$

The inductor current value is negative in this mode so there is linear decrease in the current value which can be expressed as

$$\frac{\Delta i_{Lm}}{\Delta t} = \frac{\Delta i_{Lm}}{(1-D)T} = \frac{V_L}{L_M} \quad (41)$$

From (41);

$$\Delta i_{Lm(off)} = \frac{V_L}{L_M} (1 - D)T \quad (42)$$

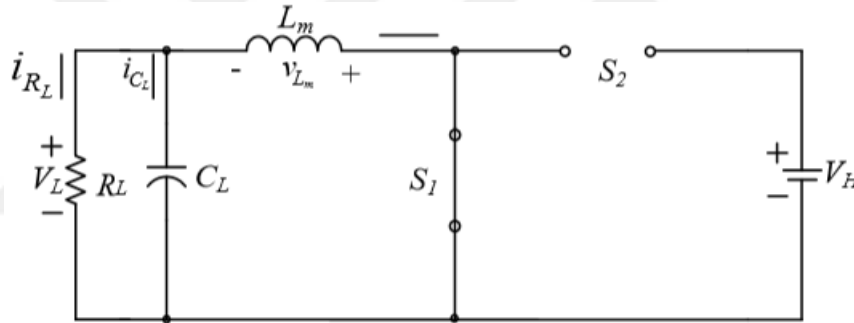


Figure 13. Buck mode of the converter when S2 is open on high voltage.

Under steady-state operation, the total change of the converter's inductor current in a single cycle of operation must equal zero, thus

$$\Delta i_{Lm(off)} + \Delta i_{Lm(on)} = 0 \quad (43)$$

From eq (38) and (42);

$$\frac{(V_H - V_L)}{L_m} DT - \frac{V_L}{L_M} (1 - D)T = 0 \quad (44)$$

Simplifying eq (44);

$$(V_H - V_L)DT - V_L(1 - D)T = 0 \quad (45)$$

This equation represents the volt-second balance principle. In addition, by further simplifying (45), the voltage relationship of the high and low-voltage sides of the converter can be determined as

$$V_L = V_H D \quad (46)$$

As shown in (3), $0 < D \leq 1$. Therefore, under this operation mode, the voltage V_L on the low-voltage side is smaller than the voltage V_H on the high-voltage side [11].

1.6.4. Component Designs of the Converter are Operated Under Buck Mode

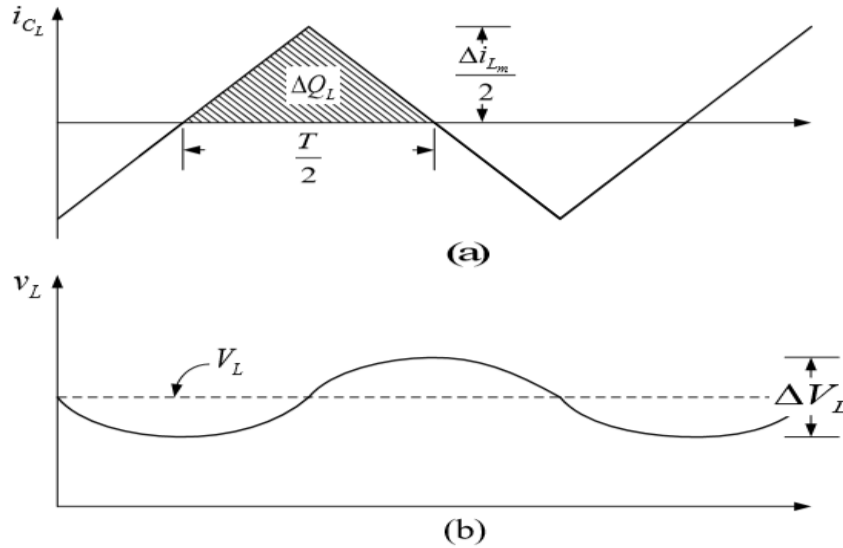


Figure 14. The waveforms of the bidirectional buck-boost converter operating under buck mode: (a) the current of the capacitor; (b) the voltage ripple of the capacitor on the low-voltage side.

The capacitance design as shown in Figure 8, the currents for capacitor CL are as follows

$$i_{CL} = i_{LM} - i_{RL} \quad (47)$$

The figure shows that the capacitor undergoes charging when the capacitor current C_L is a positive value. The Output voltage on the low side and the capacitance can be define as following.

$$\Delta Q_L = C_L \Delta V_L \quad (48)$$

By calculating the area of positive capacitor current we can find the solution for eq (49)

$$\Delta Q_L = \frac{T \Delta i_m}{8} \quad (49)$$

The voltage ripple can be calculated by simplifying (48) and (49)

$$\Delta V_L = \frac{T \Delta i_m}{8 C_L} \quad (50)$$

Substituting the value of (42) and (50)

$$\Delta V_L = \frac{V_L (1-D)}{8 C_L L_m f^2} \quad (51)$$

Where $1/F_t$ is the switching frequency. Therefore equation (51) gives the following.

$$C_L = \frac{(1-D)}{8 (\Delta V_L / V_L) L_m f^2} \quad (52)$$

1.6.4.1. Inductance Design

During buck mode the mean of the inductor and capacitor current flowing through the load resistor are identical because the mean of the capacitor current is zero under steady state condition, thus the mean value of the current can be expressed as following:

$$I_{Lm} = I_{RL} = \frac{V_L}{R_L} \quad (53)$$

From the minimum and the maximum, we can obtain the following equation

$$I_{Lm-max} = I_{LM} + \frac{\Delta i_{LM}}{2} \quad (54)$$

$$\frac{V_L}{R_L} + \frac{1}{2} \left[\frac{V_L}{L_m} (1-D)T \right] = V_L \left[\frac{1}{R_L} + \frac{(1-D)}{2L_m f} \right] \quad (55)$$

$$I_{Lm-min} = I_{LM} - \frac{\Delta i_{LM}}{2} \quad (56)$$

$$\frac{V_L}{R_L} - \frac{1}{2} \left[\frac{V_L}{L_m} (1-D)T \right] = V_L \left[\frac{1}{R_L} - \frac{(1-D)}{2L_m f} \right] \quad (57)$$

The minimum value of the inductor current must be greater than zero to operate in CCM. Thus, from the equation (57) we can obtain following:

$$V_L \left[\frac{1}{R_L} - \frac{(1-D)}{2L_m f} \right] = 0 \quad (58)$$

Thus, the minimum inductance must be satisfied from the continuity of the inductor current according to the (58)

$$I_{Lm-max} \geq \frac{(1-D)R_L}{2f} \quad (59)$$

To maintain the consistency of the inductor current flows for the bidirectional buck-boost converter when operating under boost and buck modes, (34) and (58) can be further simplified as follows:

$$I_{m-boost} = \frac{D(1-D)^2 V_H^2}{2P_H f} \quad (60)$$

$$I_{m-buck} = \frac{(1-D)^2 V_L^2}{2P_L f} \quad (61)$$

1.7. PI Controller

PI controller is the most widely used controller in industrial product as well as daily routine robust practical experiments due to its simplicity and user-friendly behavior. It is

easy to control and understand, according to survey 90% of process industries use them still just because it's easy to retune according to specific need. The PI is named as so it is the sum of three terms proportional, integral.

The proportional term is used to maximize the output so that it nearly reaches the input value, but it does not eliminate the error properly it is generally used to speed up the responses of the system so that error can be eliminated as so as possible. The integral term eliminates the offset as by the order of the system also increases the system responses but with the sustained oscillations derivative term is usually used to eliminate and decrees the oscillatory response of the system it neither changes the offset nor effects the order and type of the system. Change in the each of these properties cause the change in the system response so it is important to find out the proper value for the system so that it matches the response of the system and controls the output properly. Now a day new MATLAB version have already upgraded the system in such a way that the PI controller tunes itself according to the system.

The output of the PI controller is the combination of proportional and integral controllers.

$$u(t) = K_p e(t) + K_1 \int e(t) dt \quad (61)$$

$$U(s) = \left(K_p + \frac{K_1}{s} \right) E(s) \quad (62)$$

$$\frac{U(s)}{E(s)} = K_p + \frac{K_1}{s} \quad (63)$$

Therefore, the transfer function of proportional integral controller is $K_p + \frac{K_1}{s}$

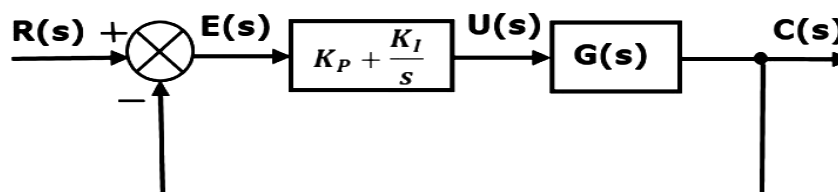


Figure 15. PI controller block diagram.

The proportional integral system is good to remove the steady state error without effecting the system stability.

1.8. Maximum Power Point Tracking – (MPPT)

The emergence of the latest power control mechanism, commonly referred to as MPPT (Maximum Power Point Tracking) algorithms has resulted in increasing the operational efficiency of the solar modules. MPPT offers an opportunity to maximize the output power of the PV array, specifically by keeping a track on the maximum power on each operating condition. Therefore, it can be affirmed that MPPTs could be effectively utilized in the renewable energy sector. The efficiency of MPPT can also be understood by considering the findings of the study of [10] according to which a typical solar panel can convert only thirty to forty percent of the incident solar radiation into electrical energy. In this situation, MPPT helps in improving the overall efficiency of the solar panel. As per maximum power transfer theorem, the power output of a circuit maximizes when the source impedance (Thevenin impedance) of the circuit equalizes the load impedance. There are several techniques that are being used for tracking maximum power. These include fuzzy logic, neural networks, fractional open circuit voltage, fractional short circuit current, incremental conductance method, hill climbing method (Perturb and Observe). It is established that the selection of optimal technique is dependent on several factors including ease of implementation, implementation cost, etc.

Considering all the benefits, the MPPT controller has been utilized. It is found that numerous MPPT algorithms have been presented by the researchers. Some of them possess highly complexed functions and some of them can be easily applied in the given scenarios. Amid all the traditional approaches, presented in the previous literature, P&O (Perturb and Observe), as well as INC or IC (Incremental Conductance), is widely been used for commercial applications. The present dissertation has made use of INC MPPT algorithm. The rationale behind this selection is associated with excellent dynamic behavior that is associated with this algorithm.

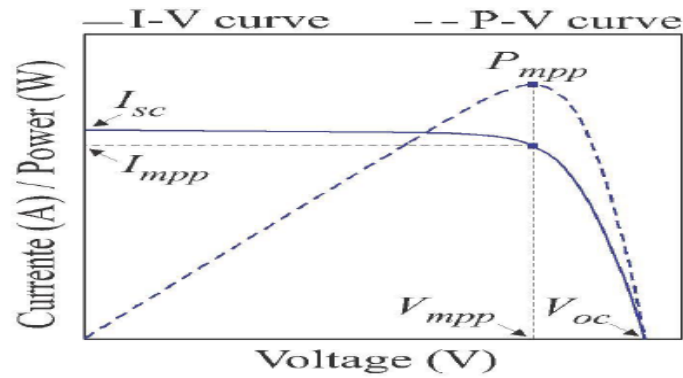


Figure 16. SPV array P-V and I-V curve [31].

It is evident from the above picture that the P_{pv} versus V_{pv} curve has a bell shape. It is also prominent in the diagram that the curve's slope is zero (at maximum power), negative (right hand), and positive (at the left hand). With the varying irradiance, I_{pv} gets changes. However, no change takes place in V_{pv} , from the start to the end of the operations. The selected MPPT algorithm has the capability of continually sensing and comparing the current and voltages with the load impedance. When the source impedance gets matched with the load impedance it is called MPP point. This functional characteristic shows that load helps in deciding the operating point. It is important to note that at this point the slope reaches the value of 'zero'. The figure 17 shows INC algorithm's flow chart.

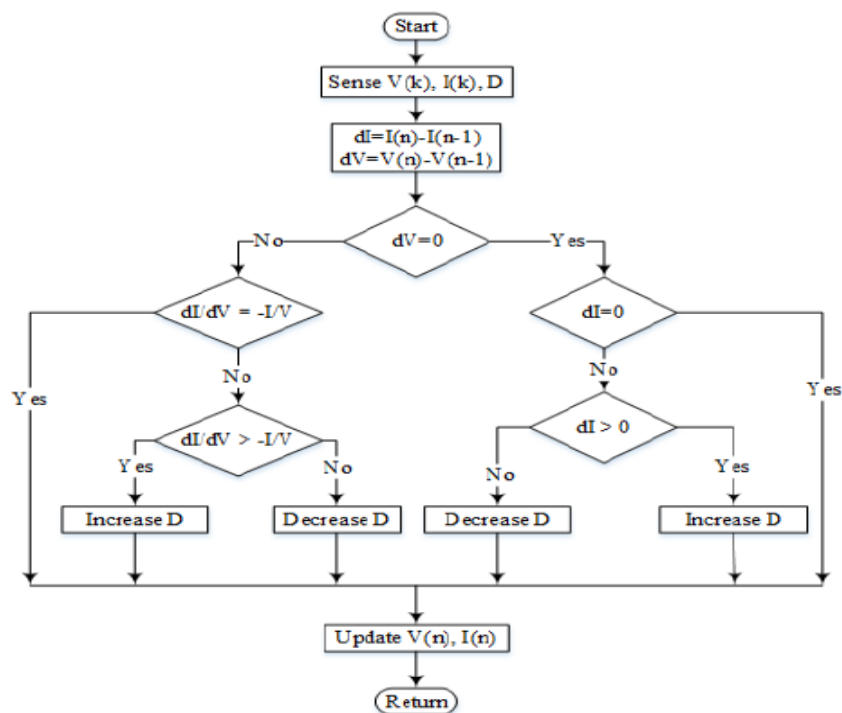


Figure 17. Flow chart - INC MPPT algorithm.

The selected MPPT algorithm is responsible for producing the duty ratio for the DC-DC converter that helps in regulating the overall power.

1.8.1. Perturb and Observe

Perturb and Observe (P&O) method is widely used among the MPPT algorithms. This method works independently from the environmental conditions. Current and voltage sensors are needed to make calculations, so that it has a higher cost relatively [22]. Basic principle of this method is to calculate the output power PPV and perturb the duty cycle by increasing or decreasing it. After every perturbation the output power is recalculated. If it is increased perturbation is repeated in the same direction otherwise direction of the perturbation reversed. This method has some drawbacks. These are; oscillations when MPP reached at steady state because of constant perturbation, slow tracking speed and wrong decisions when fast changes happen in the irradiation or temperature. In this method Increment and decrement of duty cycle is carried out by calculating output power.

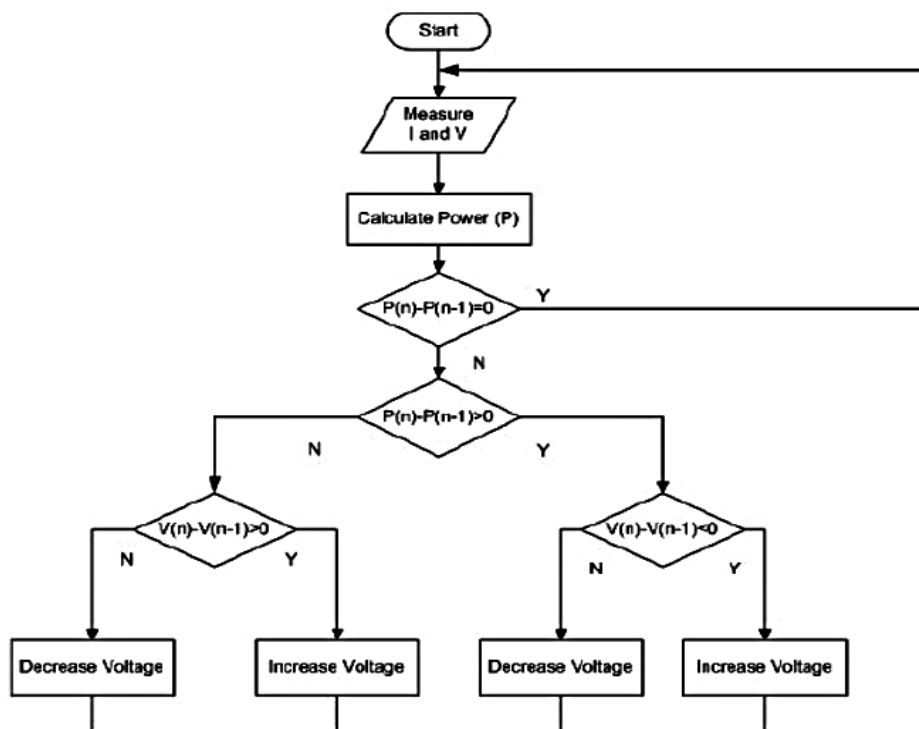


Figure 18. Flow chart Perturb and Observe algorithm

1.9. Inverter Technology

Technically inverter technology is an electronic device that is used to convert DC that is the Direct Current DC into alternating current AC.

In today's time all the electricity that we consume at home is in form of AC that is alternating current, and all the appliances that we have at home or offices are built to run on AC. But when there is a power failure or absolutely no power supply, we need backup or stored power to run to run these appliances or to simply to get electric supply. This is the point where the idea of batteries was brought up by humans that could store energy that could be used whenever needed. But the issue that rises here was that a battery can only store direct current while the electricity that is required needs to be in AC.

To resolve this issue, we need special device that could convert DC into AC. And that's where Inverters technology came in, that converts the energy stored in batteries that's in DC into AC that's required by appliances.

A basic inverter is used to convert direct Current (DC) into alternating current (AC) but inverters can be found in various types and kinds based on different parameters. For example, they can be classified based on how the power electronic switches are arranged that can be further be classified into two types that are half bridge inverters and full bridge Inverters.

1.9.1. A Full-Bridge Inverter

It is having two legs that consist of two switches that are semiconductor and load connected at the center points of both the legs.

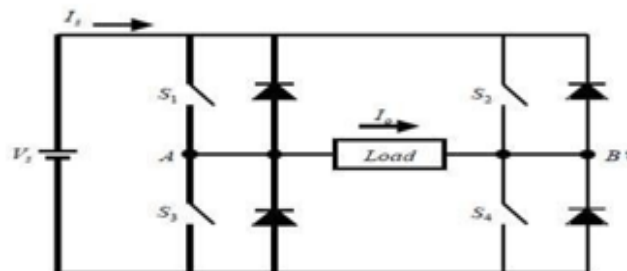


Figure 19. Full Bridge Inverter Circuit.

As we can see in Figure 19 four switches (S1, S2, S3, S4) that are semiconductor are arranged while the load connected with both legs the switched are arranged in the form of the letter H. Hence, it is also called the H-bridge Inverter. All switches are provided with the feedback diodes. DC source V_s has been connected to the H-Bridge. All four arranged switches can be in switched in 3 different sequences:

- When two switches S2 and S3 are switched on $-V_s$ is obtained as the outcome.
- When the other two switched S1 and S4 are switched on $+V_s$ is obtained as the outcome.
- When all four switches S1, S2, S3 and S4 are switched on altogether Zero voltage is obtained as the outcome.

1.9.2. Pulse Width Modulation

Differences in duty cycle of the PWM signals provide voltages across the load in a pattern will be visible on the load as the AC signal. After passing the signal through a low pass filter a pure sin wave will be acquired. The pattern at which the duty cycle of PWM signal differs can be executed using digital microcontroller or analogue components. The output of the Inverter is controlled by the sinusoidal PWM that is generated by either of the two basic topologies.

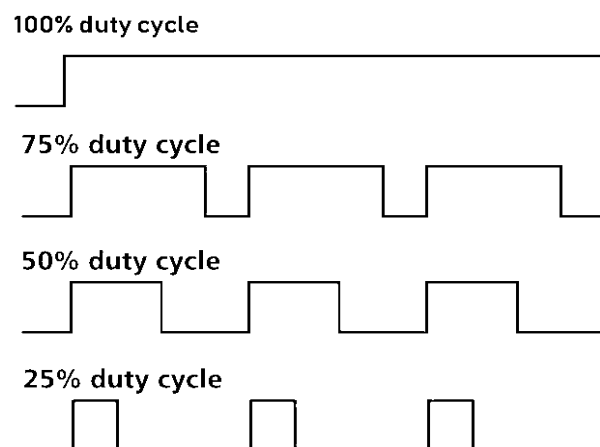


Figure 20. PWM with different duty cycle of modulated signal.

PWM signals are widely applied and used in modern day technologies such as the appliances. Some of the examples are:

- Easy to generate.
- Reduced power loss.
- Digital to analogue conversion.

The wanted PWM technique must have these characteristics:

- Voltage control linearity.
- Enough time allowance for operation of the switches and control system.
- Low switching losses in switches.
- Minimize the harmonic content of output current.
- High voltage gain-good utilization of Direct current supplies.

Two signals are compared in (Sinusoidal Pulse Width Modulation) SPWM. The carrier wave is triangular, and the modulating reference signal is sinusoidal. Gating pulses are produced by comparing the two signals and the width of each pulse varies in proportion to the amplitude of the sine wave. The inverter's output frequency is determined by the frequency of the reference signal and the modulation index and the RMS value of the output voltage is controlled by the reference peak amplitude.

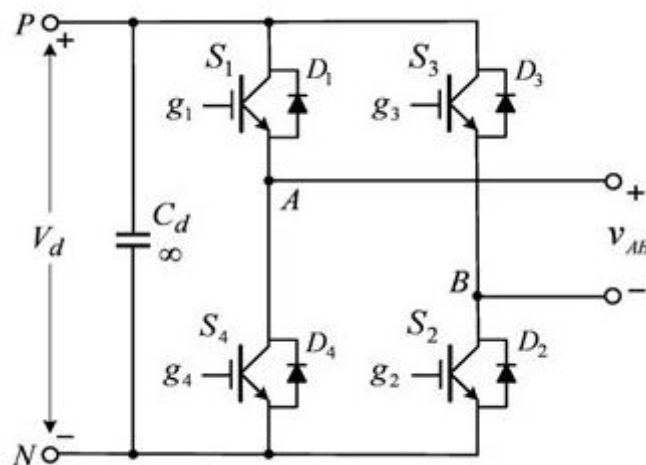


Figure 21. Single phase H-Bridge inverter [30].

For both the schemes, the H-bridge inverter circuit remains the same. We can consider H-bridge circuit that comprises the IGBT switches for both unipolar and bipolar Inverters as can be seen in Figure 21.

1.9.3. Unipolar Inverter

There are two sinusoidal waves in unipolar modulation technique with 180° out of phase. These two sinusoidal waves are compared with the triangular wave to generate the switching signal for the switch S1 and S3. The upper two switches are not switching simultaneously which is the main difference between unipolar and bipolar modulation. In bipolar modulation all the switches are switching same at the same time. In unipolar modulation the output voltage is switching between zero to positive half cycle $+V_d$ or between zero to negative half cycle $-V_d$ which gives reduce switching losses. Over modulation happens when the modulation index is greater than unity.

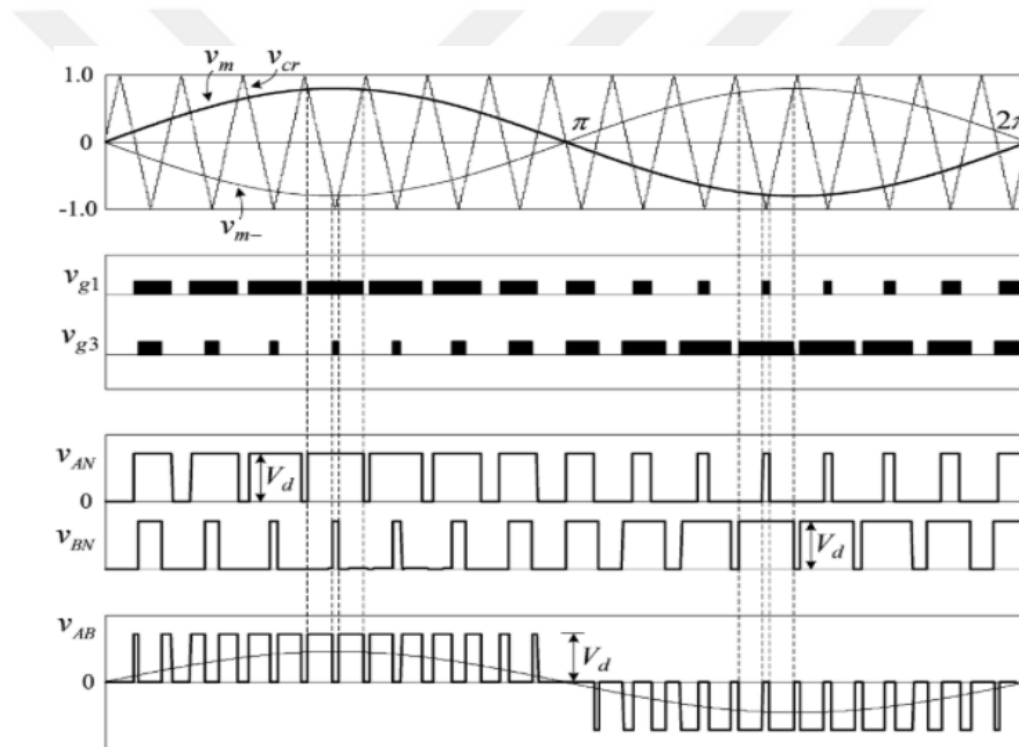


Figure 22. Waveforms of unipolar modulation scheme [30].

1.10. V/F Control Based Scalar Control

Scalar control is based on the steady state model of the motor. The control is due to the magnitude variation of the control variables only and disregards the coupling effect in the machine. For example, the voltage of a motor can be controlled to control the flux, and frequency or slip can be controlled to control torque. However, flux and torque are also

functions of frequency and voltage respectively. This method is simple and easy to implement, but the inherent coupling effect (i.e. both torque and flux are functions of voltage or current and frequency).

$$V = 22 \times \pi \times f \times N1 \times \phi \times K_w \quad (64)$$

Here ϕ = stator flux

$N1$ = stator turns

V = stator supply voltage

f = supply frequency

K_w = winding factor

$K_w = K_p \times K_d$

n^{th} Harmonic pitch factor

γ = slot angle

$$K_{pn} = \cos \frac{n\alpha}{2} \quad (65)$$

n th harmonic distribution factor;

$$K_{dn} = \frac{\sin \frac{mny}{2}}{m \times \sin(n\lambda)} \quad (66)$$

Where short pitch angle for the elimination of n th harmonics;

$$\gamma = 180 \times \frac{\text{pole}}{\text{slots}} = \frac{\text{No of slots}}{\text{pole} \times \text{phase}} \quad (67)$$

From equation 64 it can be deduced that,

$$\phi \propto \frac{V}{f} \quad (68)$$

V/F ratio must be constant for ensuring inductor motor's flux operations. Since the speed is extremely low at the starting stage, the voltage should also be low to ensure constant

flux operation. Equation number 73 demonstrates the characteristic of the centrifugal pump, depicting relation of speed and power or speed and torque. As per the provided relationship (equation), the operating speed is dependent on the power that is given from the input side. These settings will produce frequency reference as well as modulation index for V/F control. Φ is responsible for controlling reference sinusoidal wave's frequency.

$$\varphi = \int \omega^* dt \quad (69)$$

$$V^* = \alpha \times \sin(\varphi) \quad (70)$$

Here,

α = modulation index

Following steps can be taken for the generation of the reference speed.

$$V_r = V_{dc}^* - V \quad (71)$$

The speed error is generated when the error voltage crosses the PID controller.

$$\omega_{r(n)} = \omega_{r(n-1)} + K_P \times \{V_{r(n)} - V_{r(n-1)}\} + K_I \times V_{r(n)} \quad (72)$$

The speed of the pump can be given as:

$$\omega_{pump} = K_p \sqrt[3]{P_{pv}} \quad (73)$$

On the other hand, the reference speed can be written as:

$$\omega^* = \omega_{pump} + \omega_r \quad (74)$$

1.11. Single Phase Induction Motor

When three-phase and single-phase induction motors were assessed it was established that the characteristics of both motors are similar. However, there is one distinction that single phase motors do not possess a starting torque. In order to make it self-start, certain

measures must be taken. Induction motor starter is given with a supply of single-phase sinusoidal waves that result in the production of such sinusoidal alternating flux that has a synchronous speed. It is found that the sum of synchronous speeds' opposite and equal flux. The outcome is the stator flux that is shown as follows' [4]

$$F_s = F_{s,max} \sin \omega t \times \cos \alpha \quad (75)$$

$$F_s = \frac{1}{2} F_{s,max} \sin(\omega t - \alpha) + \frac{1}{2} F_{s,max} \sin(\omega t + \alpha) \quad (76)$$

As a result of this flux, opposite torque is produced. Moreover, it also leads the resultant torque to research the value of “zero”. In this way, it can be articulated that the single-phase induction motor has “zero” starting torque.

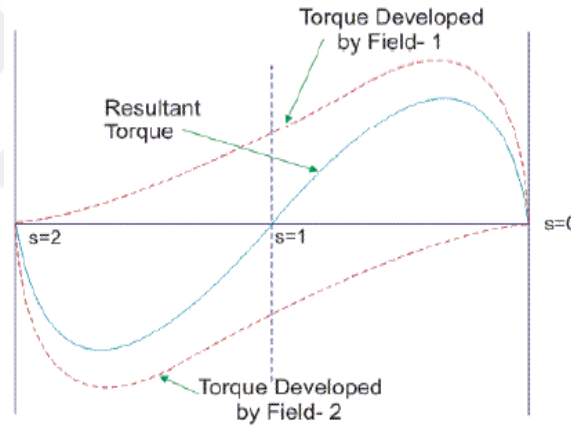


Figure 23. Single-phase induction motor – torque-slip characteristics [39].

However, the resultant torque can be positive if the rotor is rotated or moved in the forward (anticlockwise) direction. It is due to the fact that in this situation, the backward torque is less than the forward torque that eventually gives the positive value of the resultant torque. Likewise, the acceleration of the motor is in a forward way, with backward torque less than the forward torque; thereby, yielding the positive resultant torque (due to the forward direction of the motor). It is significant to bring into the notice that the speed of the motor is calculated by the torque supplied on load while considering mechanical and other types of losses.

The motor's synchronous speed can be written as:

$$N_s = \frac{120 \times f}{p} \quad (77)$$

Slip attained due to Sf (forward field) can be written as:

$$s_t = \frac{N_s - N_r}{N_s} = s \quad (78)$$

Slip attained due to Sb (backward field) can be written as:

$$s_b = \frac{N_s + N_r}{N_s} = 2 - s \quad (79)$$

Here,

f = supply frequency (Hertz) s = induction machine slip

p = total number of poles in induction motor

The diagrammatic representation of the single-phase induction motor's equivalent circuit is presented as follows:

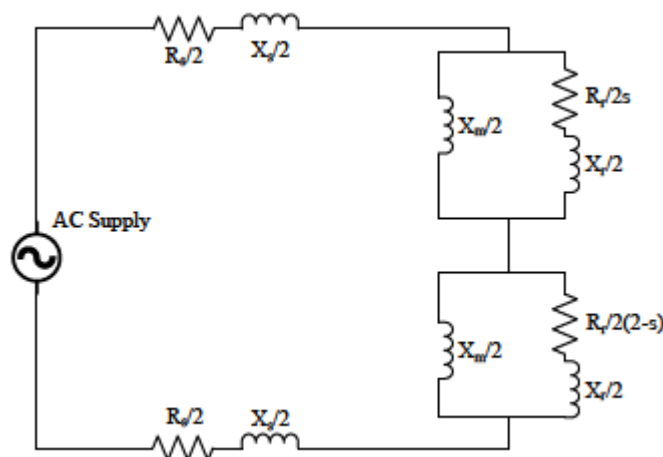


Figure 24. Single phase induction motor equivalent circuit.

For making it applicable to the water pumping system, the induction motor is attached to the centrifugal pump. More often, single phase induction motor possesses the efficiency of 64%. There are a number of techniques that have been formulated for initiating the

operations of the induction motor. However, the present research work has taken capacitor start machine into consideration so as to ensure smooth operations of the induction motor. In this regard, the main and auxiliary windings are interconnected through the help of a centrifugal switch. It is important to note that the connection of the centrifugal switch with the main circuit will be detached when motor's speed will be 70 or 80 % of the synchronous speed. The whole mechanism is illustrated as follows:

$$\tan^{-1} \left[\frac{X_m}{R_m} \right] + \tan^{-1} \left[\frac{X_A - X_C}{R_A} \right] \quad (80)$$

$$C = \frac{1}{\omega X_C} \quad (81)$$

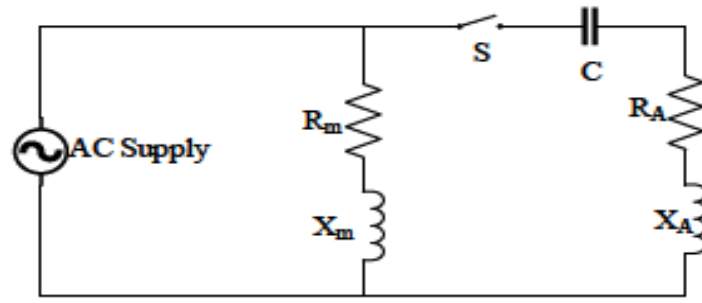


Figure 25. Circuit diagram of capacitor start induction.

Motor Here,

X_m = Reactance of main winding R_m = Resistance of main winding

X_A = Reactance of auxiliary winding

R_A = Resistance of the auxiliary winding

C = Capacitance required for the development of the 90-degree angle amid auxiliary and main winding to produce maximum starting torque.

The intercoupled system having a centrifugal pump as well as induction motor has been used for water pumping. It is significant to bring into the notice that a centrifugal pump's design is developed on the basis of pump affinity law. As per this law, the load torque has a proportionality with the square of speed.

$$T_L = K_p \times \omega_r \quad (82)$$

$$K_p = \frac{9.94}{(2 \times \pi \times 24)^2} = 0.00043712 \text{ Nm/rad} \quad (83)$$

Motor parameters are as following;

2000W 4-Pole, 1440 rpm, 50Hz, Main Winding Stator Resistance- 0.602Ω , Inductance 7.4mH , Rotor Resistance- 1.012Ω Inductance- 5.6mH ,Auxiliary Winding Resistance- 7.14Ω , Inductance- 8.5Mh .



2. CASE STUDY AND METHODOLOGY

2.1. PV Array Design

The PV system used here is built in PV array block by MATLAB Simulink. There are several blocks available according to their specifications. The block which we used here is Trina solar PV array which consists of 2 parallel and 4 series connected modules. The irradiance graph for 1000 and 500 value is given in the figure 25.

The parameters of the single PV array are as given below;

- Open circuit voltage V_{oc} (V) = 44.3
- Short circuit current I_{mp} (A)=8.25
- Voltage at maximum power output V_{mp} (V) = 35.5
- Cells per Module = 72
- Current at maximum power output I_{mp} (A) = 7.6
- Maximum Power (W) = 269.8

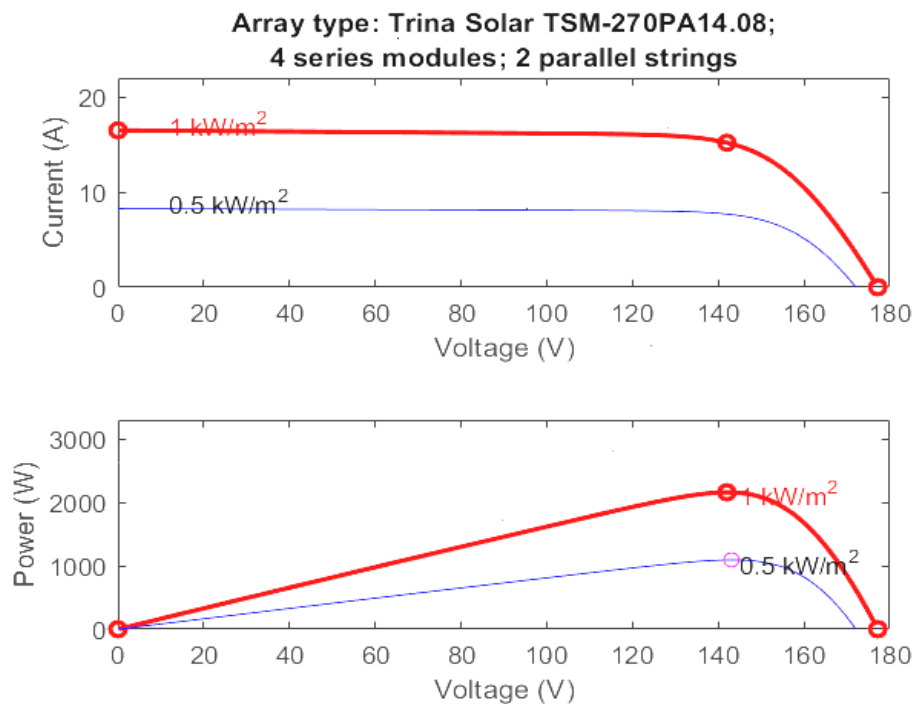


Figure 26. Power and Current output of PV

2.2. Design of DC-DC Converter

The DC /DC converter we used here is a boost converter as per requirement our main purpose is to maximize the output voltage in such extent so that we can utilize it in a proper manner for our inverter process. We have briefly discussed the working principle of boost inverter in above chapter before here the Simulink diagram is mentioned above.

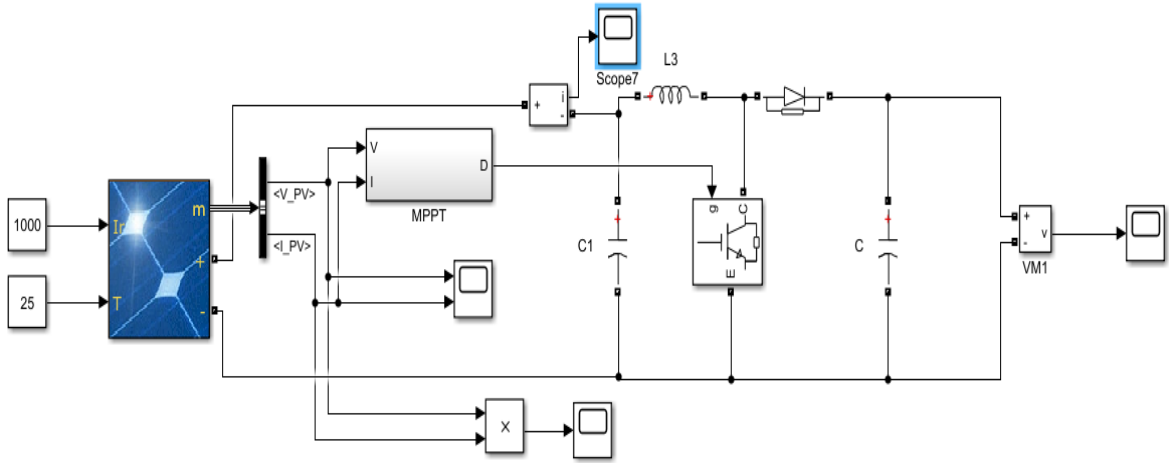


Figure 27. Boost converter circuit diagram.

The specification of the electronic components used above are as follow

$$D = \frac{V_{dc} - V_{mp}}{V_{dc}} = \frac{350 - 177.2}{350} = 0.4937 \quad (84)$$

$$L = \frac{V_{mp} \times D}{\Delta I_L \times f_s} = \frac{177.2 \times 0.4937}{0.2 \times 9 \times 20000} = 2.43 \text{mH} \quad (85)$$

$$\frac{1}{2} \times C \times [V_{dc}^2 - V_{dc}^2] = \alpha \times V \times I \times t \quad (86)$$

$$\frac{1}{2} \times C \times [305^2 \times 325.26^2] = 1.2 \times 230 \times 9 \times 0.005 \quad (87)$$

$$C = 1486.897 \mu\text{f}$$

Input Capacitor (c) = 100uf

Inductor =2mH

Output capacitor=1500uf

The boosted output of the converter is needed to be maintained at a constant value for that purpose a well-defined duty cycle is needed which can be given by MPPT maximum power point tracking system or by the PID controller. The solar panel we used here consist on 3 cells in parallel and 4 cells in series maximum power can be extracted up to 3238w and maximum current could be 15amp. The purpose of this converter is to extract power and current somewhere near to maximum value according to the need. Here the designed converter extracted the constant voltage up to 325 volts and the power of almost 3238w which is enough to run the SPID motor and the water pump in different irradiance situations.

2.3. MPPT Design

The MPPT system is designed so accordingly the traditional INC (Increment Conductance) method the flow chart is already given previous detail in thesis, here is the implementation of that flow chart. Here the inputs are taken from the PV cell which are then processed according to the flow chart system via increment and decrement in the current and voltage curves in order to set a specific maximum power point which defines the PV system power and required output voltage in a stable form to operate the inverter

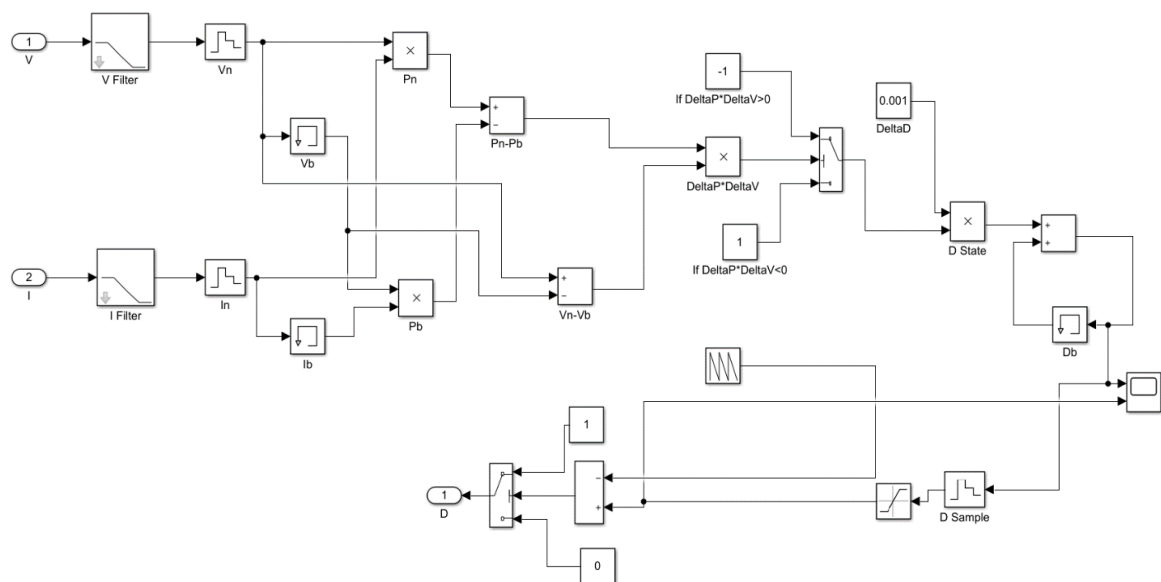


Figure 28. MPPT controller mode.

2.4. Design of Buck-Boost Converter

In the design above for the buck boost converter the arrangement of the switches is in such way that one acts as a boost and the other acts as the buck converter. The output voltage is fed to the boost converter attached to the PV array to feed inverter. According the figure above two PI controllers can be seen easily which acts as feedback controllers in order to control the voltage for buck and boost converter that's why they are used separately for each. The battery we used here is of 48volt battery whose initial charging state is 60%. At the start when switch S1 is acting as a boost converter there is a gradual increase in the battery voltage and also it shows discharging process with the increase in the inductor current after it reaches the required 325V with any further increase cusses the switch S2 to be closed and starts acting as a buck converter and vice versa battery starts charging in this mode with the decrease in inductor current. The switching frequency is 40KHz and the not logic gate indicates the inverse of the signal for opposite switch.

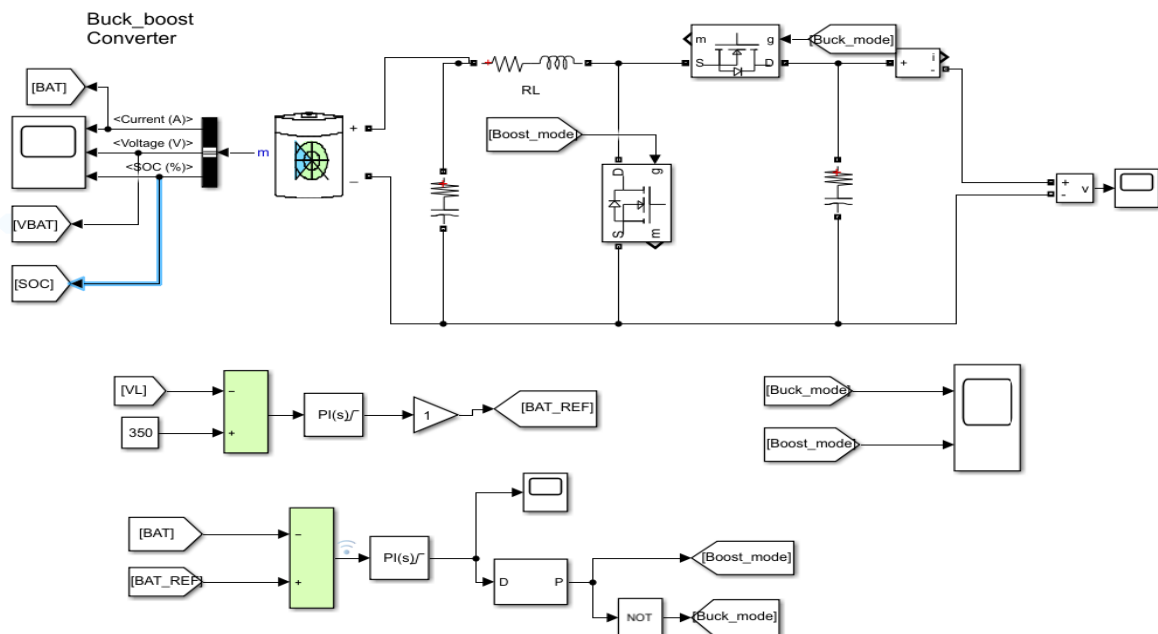


Figure 29. Buck-Boost converter.

The component parameters of the system are given as following

- Input Capacitor (c) = 1000uf
- Inductor = 1mH
- Output capacitor=1000uf

2.5. Single Phase Inverter with Controller

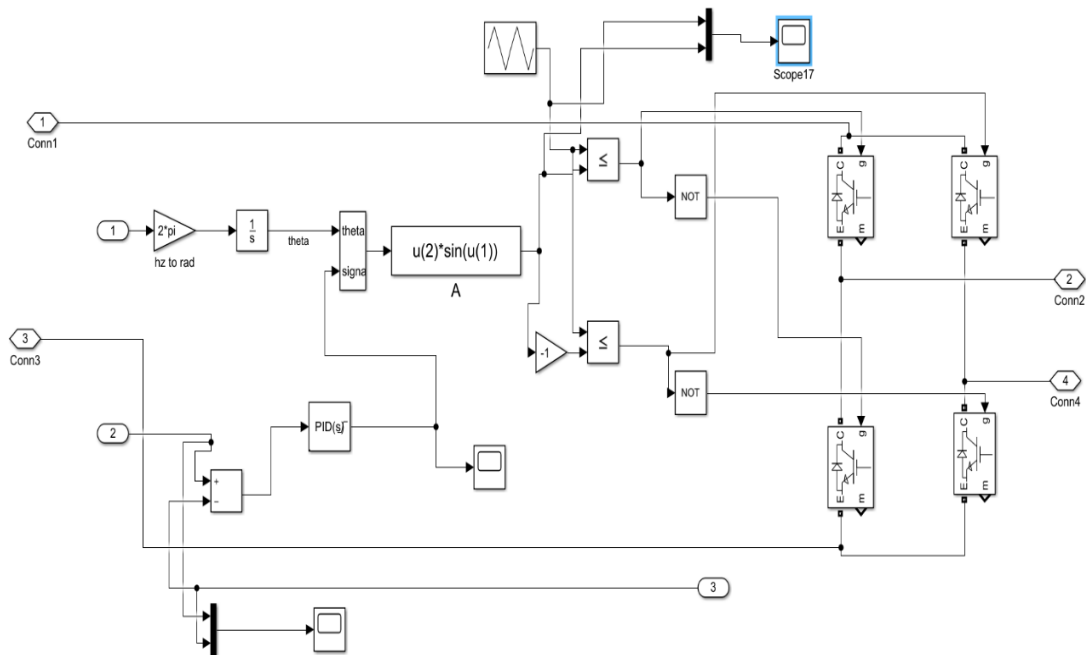


Figure 30. VSI circuit diagram.

The inverter used here is a classic 4 switch inverter uses MOSFET switches consisting on parallel diodes for the freewheeling time period to avoid the switching losses they are connecting back to back and in a parallel arrangement. Single phase pulse modulation is used to switch the MOSFET. To achieve the desire modulation a MATLAB sine wave function block is used which is given two inputs, one is frequency and the other is Voltage which creates the modulation index. Here the modulation index plays the important role in the modulation strategy.

According to per requirement the specific voltage at the output is controlled by the modulation technique used where frequency and the modulation index are the key factor. The modulation index is changed from 0 to 1 which controls the magnitude of the voltage output and the frequency input controls the frequency of the sin wave by using a carrier frequency which is given by the carrier repeating signal whose frequency is equal to 20000Hz. This cause the fast switching process to achieve the desired modulation. Both legs are switch in such a way that the output voltage between the leg A and B is equal to the input voltage given by PV array well after conversion this DC supply gives the AC output.

2.6. Design of V/F Based Scalar Controller

This scheme is defined as volts per hertz control because the voltage applied command is calculated directly from the applied frequency to maintain the air-gap flux of the machine constant. In steady state operation, the machine air-gap flux is approximately related to the ratio V_s/f_s , V_s/F_s where V_s is the amplitude of motor phase voltage and F_s is the synchronous electrical frequency applied to the motor. It is the main building block of this system. To control the motor speed we must take care of keeping the torque constant so for that purpose variation of voltage and frequency should be in such a way that it doesn't affect the motor torque, as from the parameters of motor it is clear that the change of speed of motor is directly proportional to its frequency, for example if the motor is running with speed of 1800rpm its frequency should be equal to 60Hz same as it would be 900 rpm if its frequency is equal to 30Hz, half of the full frequency for the case with the voltage change it is same. In overall system the voltage and frequency should change according to each other from the maximum to minimum frequency which could be done by only V/F control system.

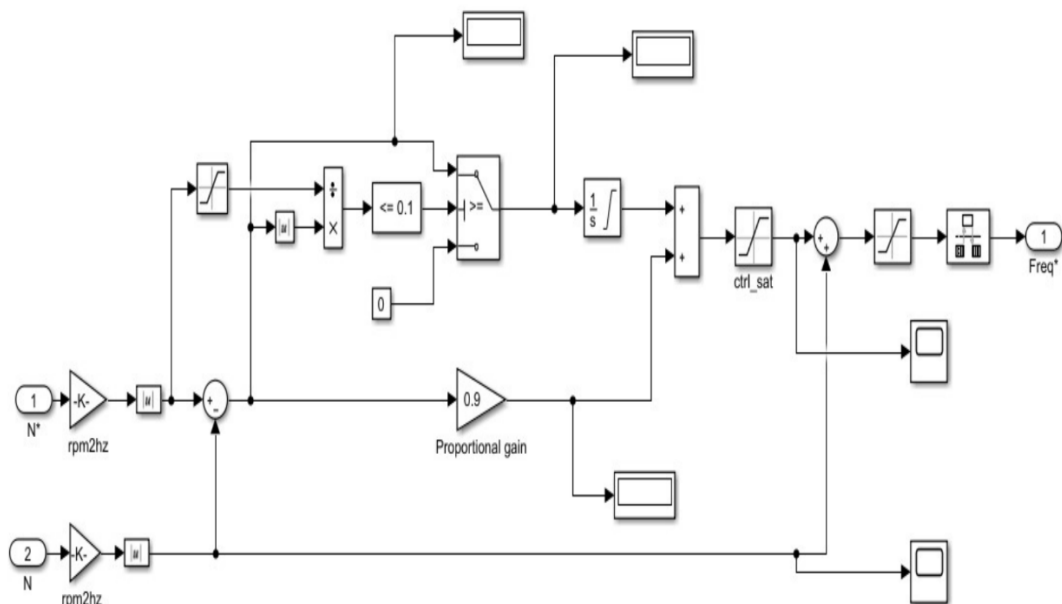


Figure 31. Closed loop PI controller mode.

The graph in the figure 32 shows the frequency and voltage relation. Frequency starts from the minimum value of 20Hz and then for the maximum speed it goes till 65Hz. It is cleared from the graph of figure 32 that after 50Hz there is no change in voltage as the required voltage for the motor is maximum 230V.

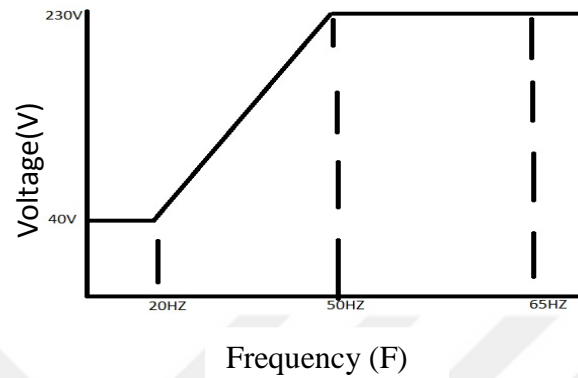


Figure 32. Voltage and frequency relation for the motor speed control.

We used the MATLAB function block to write the code to develop V/F relation. It is given as following:

```
function V = fcn(F)
V=0;
Fnom=50;
Fmin=20;
Fmax=65;
Vmin=40;
Vmax=230;
if (F<=Fmin)
    V = Vmin;
elseif (F<Fnom)
    V = (((Vmax-Vmin).*(F/Fnom))) + Vmin;
elseif (F>=Fnom)
    V = Vmax;
End
if (F>=Fmax)
    F=Fmax;
```


2.8. Main Topology Circuit Design Without Controller

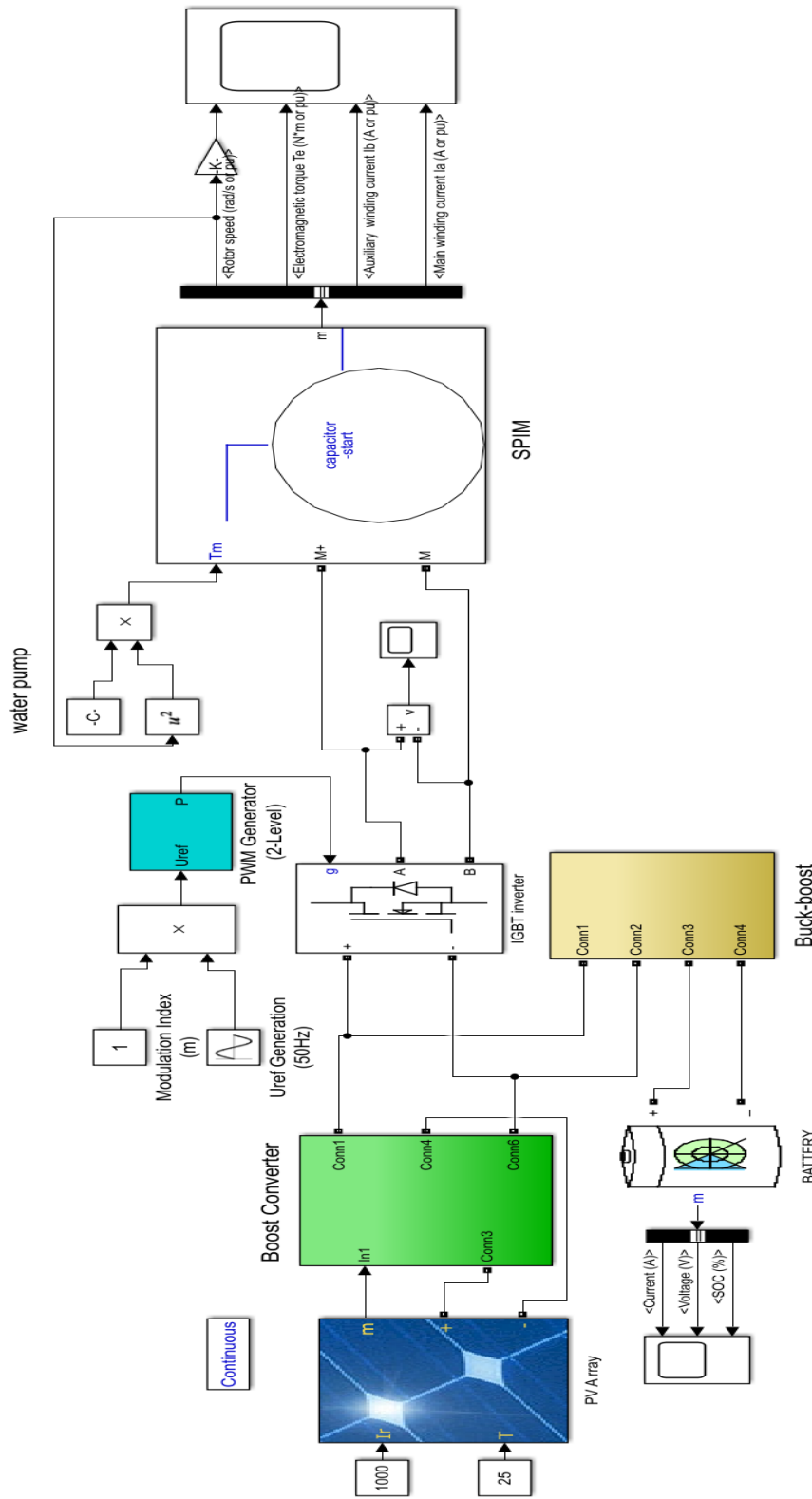


Figure 34. Buck-Boost converter fed controlled water pumping system circuit design without controller.

The main system design consists of single-phase induction motor. Its main winding is connected through the inverter output which gives the voltage input to the motor. Output voltage of the inverter is controlled by the v/f scalar control system which gives the defined modulation index to control the magnitude of the sine wave in order to get the required output voltage. The speed of the motor is controlled by the closed loop PI controller which is given the reference speed. The closed loop PI controller compares the reference speed with the machine output speed and minimizes the error to get almost zero output for the controller error. The centrifugal pump is taken as the Torque load which is equal to $K_p=9.37$. As the machine starts the load starts increasing with the increase in speed and reaches to the maximum value for the given K_p . The main purpose of this system is to make induction motor running with the required reference speed which is given here as 1300rpm and then it changes to the reference of 1500rpm which is the maximum speed achieved by the motor.

3. RESULTS

All the results are explained via graphical form and with their required tags for the operation. The MATLAB/Simulink results are given with the change in irradiation with the time, charging and discharging points of the battery are also mentioned. The results below also show the comparison of the induction motor speed with controlled and without controlled in terms of MATLAB/Simulink.

3.1. Simulation Results of PV Array

In this section all the results obtained by the PV array via boost converted and the buck-boost converter are shown in MATLAB/Simulink and discussed with given values. Experiments are performed by changing irradiance of the PV array. All results are taken for the time period of 10 seconds.

3.1.1. Voltage Output of DC Bus Without Speed Control of Motor

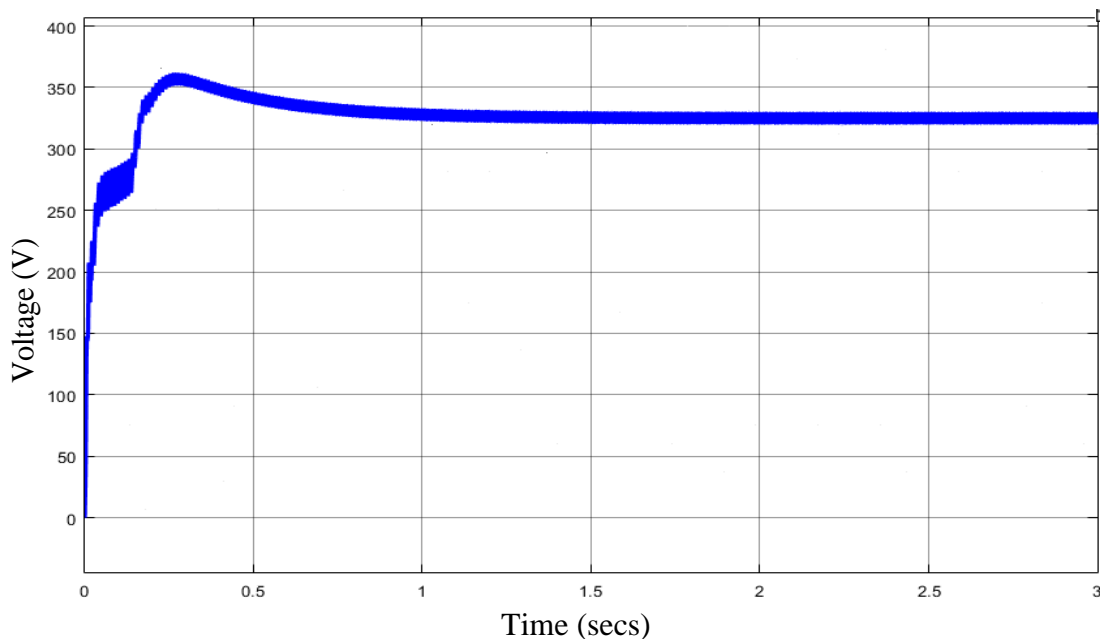


Figure 35. DC bus voltage output.

In the figure 35 the voltage output of the boost converter is stable at 325V with no change in speed of the motor shows that there is no fluctuation in the voltage waveform. It stays stable thorough out the process the buck-boost converter supports the Boost converter in order to maintain the voltage stability and to charge and discharge the battery. This voltage is later given to single phase inverter to convert DC to AC in order to feed the induction motor where 230rms voltage is required to run the motor with maximum speed.

3.1.2. The Voltage of the DC Bus With Speed Control of Motor

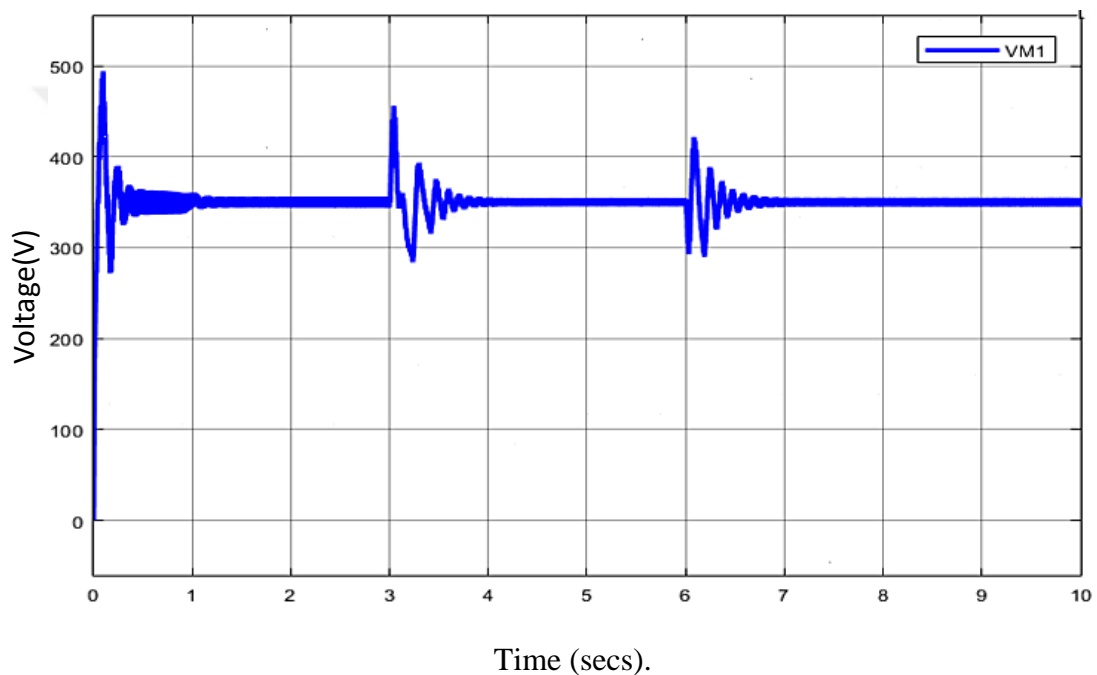


Figure 36. Voltage output of boost converter.

In the figure 36 the voltage output of the boost converter is shown. The control mechanism is applied via PI controller to control the voltage output at 350V in order to run the motor smoothly with the variation in speed input. It can be clearly seen in the above figure that there is a variation in the voltage output at different time in seconds over the entire 10sec output. When the speed is changed to 1000Rpm at the time of 3sec the PI controller sets the output again at 350V via feedback. The same process repeats itself at the time period of 6sec and again PI controller stabilize the voltage output at 350V. Due to continuous voltage control motor runs smoothly with different input speed at any time period and it also causes the charge and discharge of the battery.

3.2. Simulation Results of Inverter Output Voltage

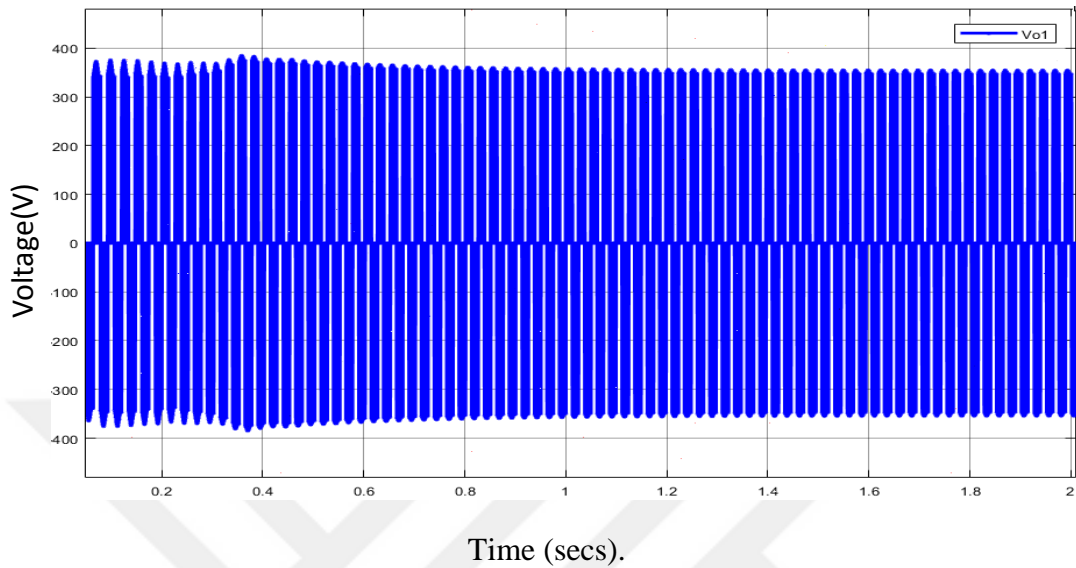


Figure 37. Inverter voltage across leg A and leg B

In the figure 37 the voltage output of the inverter is shown across the leg a and leg b. Value of the voltage is 350V. The bar of the voltage goes from zero to positive 350V and again from zero to -350V according to single phase inverter unipolar modulation rule.

3.2.1. Simulation Result of Sinusoidal Output Waveform

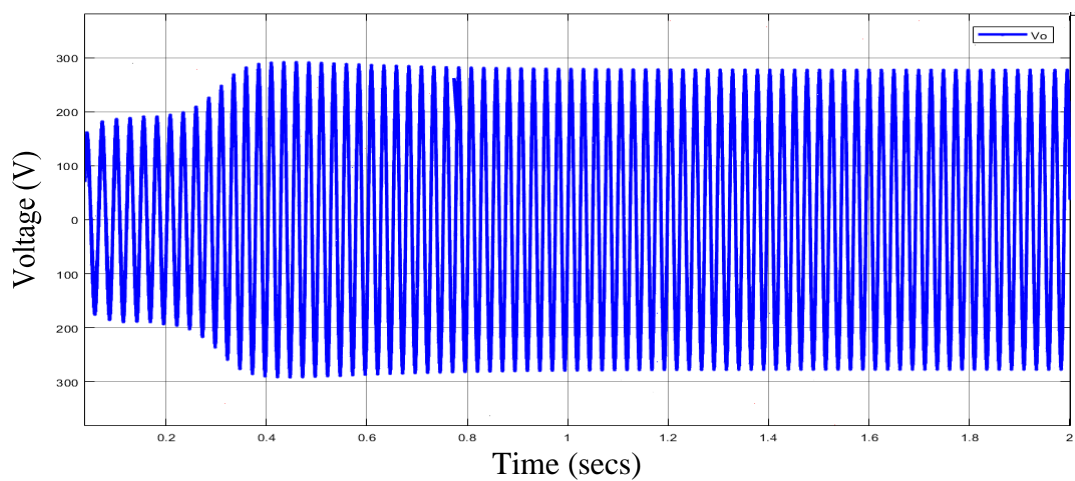


Figure 38. Sinusoidal voltage output.

Figure 38 is zoom output result of inverter sinusoidal voltage output waveform with the 230Rms voltage.

3.3. Power Output Result of PV Array

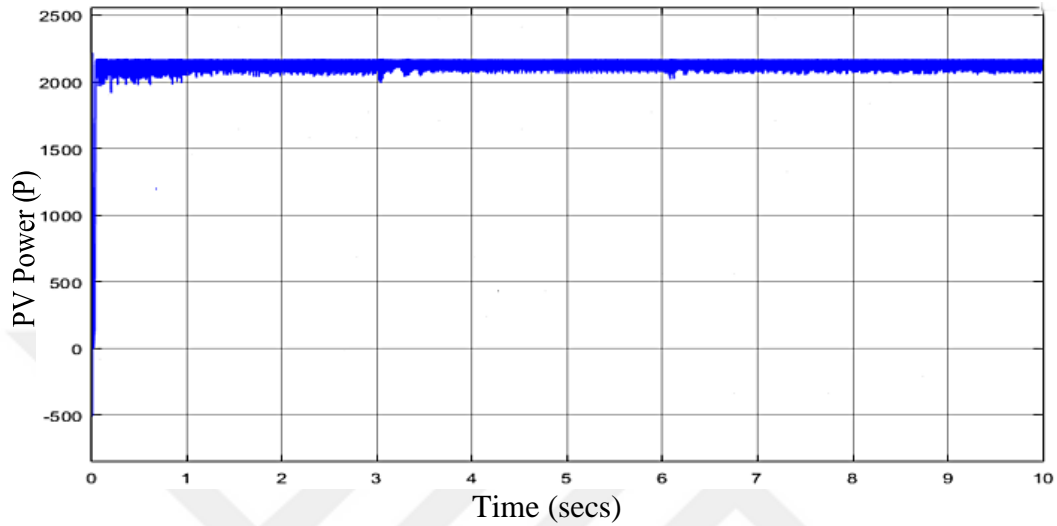


Figure 39. Power output PV array.

Figure 39 is the power output result of PV array controlled with MPPT at $1000 \text{ W}/\text{m}^2$ irradiance and 25C^0 temperature.

3.3.1. Output Waveform of PV Current and Voltage

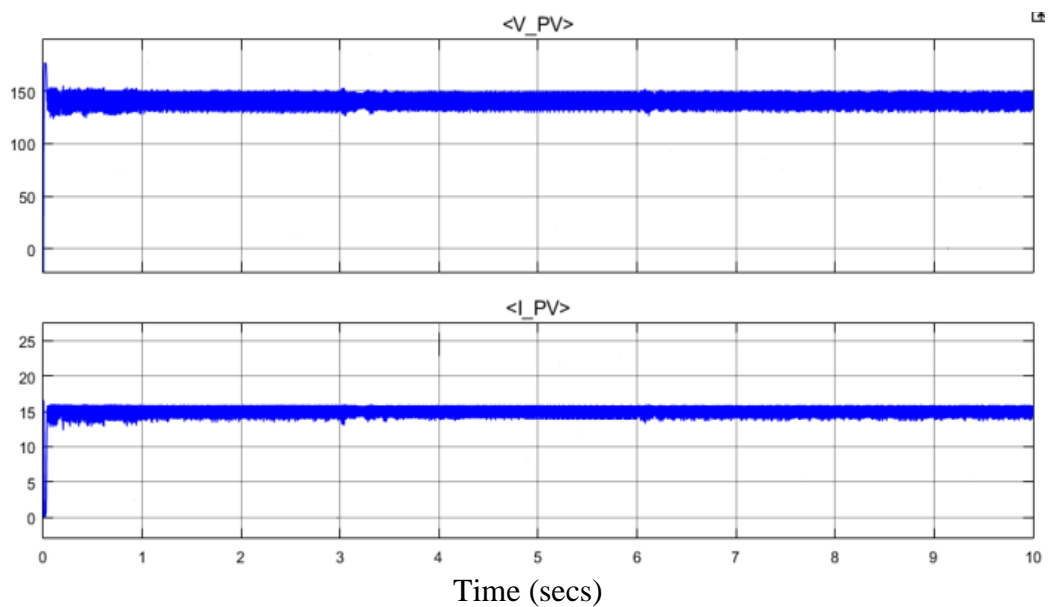


Figure 40. PV current and voltage waveform.

Figure 40 is the voltage (V_{PV}) and current (I_{PV}) output results of PV array controlled with MPPT at 1000 W/m^2 irradiance and 25C^0 temperature.

3.3.2. Simulation Results of PV Array with Change in Irradiance

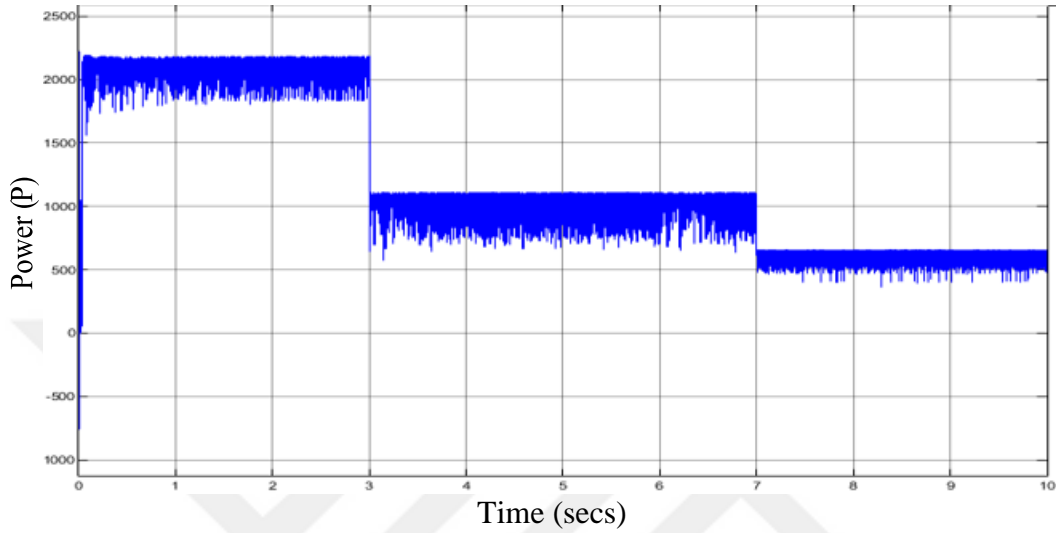


Figure 41. PV Power output

Figure 41 is the power output result of PV array controlled with MPPT at 1000w/m^2 , 800W/m^2 and 500W/m^2 irradiance and 25C^0 .

3.3.3. Simulation Result of PV Output Voltage and Current

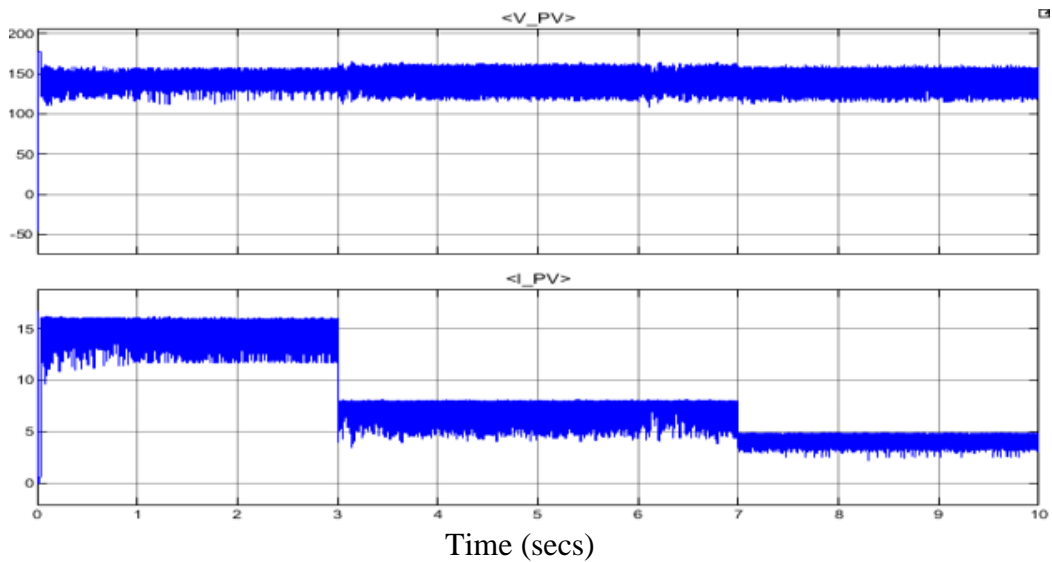


Figure 42. PV current and voltage waveform.

Figure 42 is the voltage (V_{PV}) and current (I_{PV}) output results of PV array controlled with MPPT at $1000W/m^2$, $800W/m^2$ and $500W/m^2$ irradiance and $25C^0$ temperature.

3.4. Simulation Results of Battery Output with Change in Motor Speed

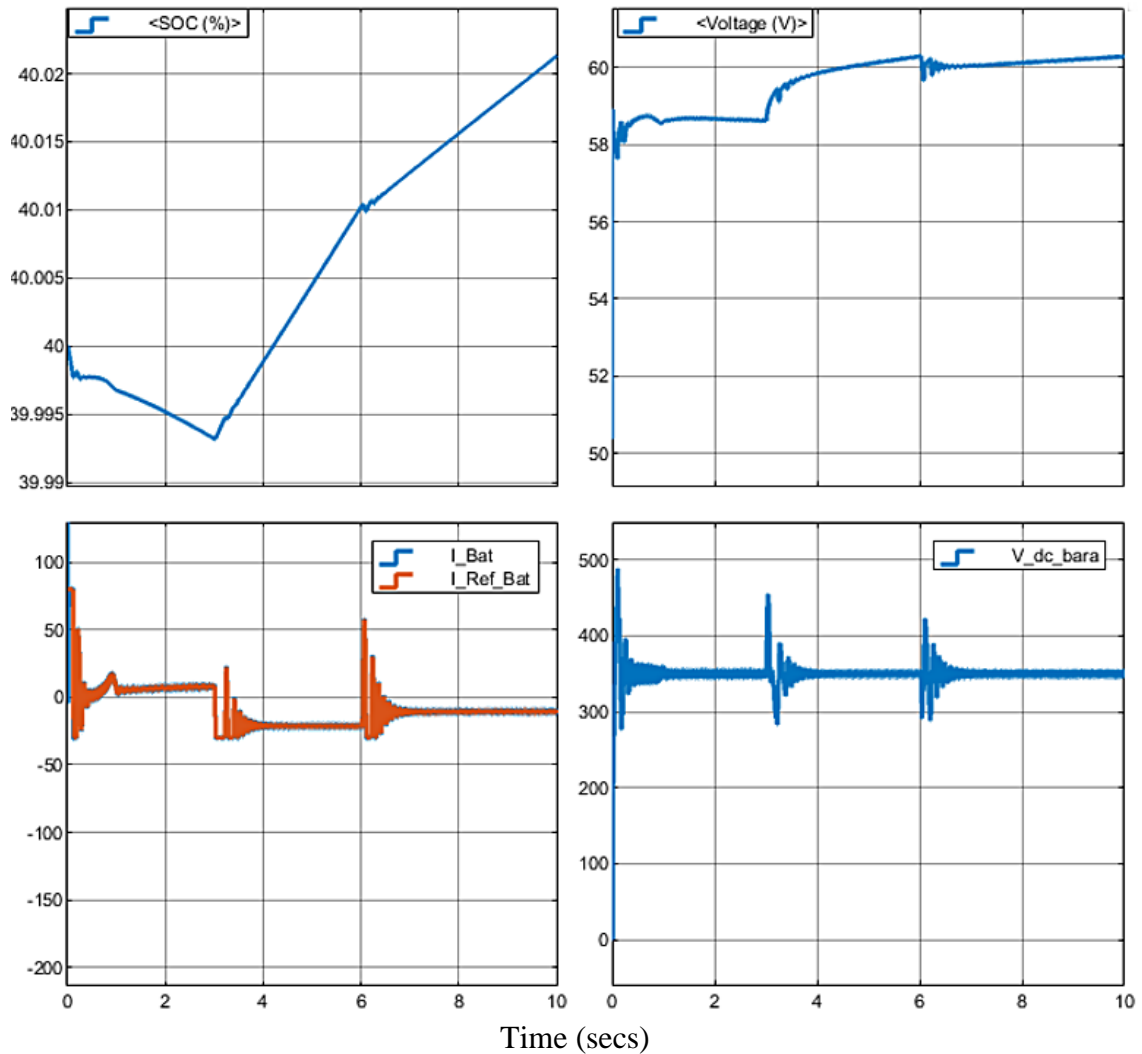


Figure 43. Battery output (a) Charging and discharging mode (b) Battery voltage (c) Battery current (d) Battery voltage

In figure 43 there are the combination of four different result outputs of the system. In the first figure the result of the state of charge (SOC) of the battery is given. From the time period of zero to 3sec battery shows continuous discharging at the 1600Rpm of motor speed and when the speed goes down to 1000rpm the battery starts charging till 7sec, again from 7sec to 10sec battery keeps on charging with the increase in speed to 1300Rpm.

In the second figure at the right battery voltage keeps on increasing from zero to 10sec but among the intervals of speed change and charging and discharging of the battery the voltage increment is little more while charging of the battery as compare to discharging.

In the third figure from the left down battery current is shown with the reference value of the controlled battery current via PI controller which keeps on following the output battery current of the buck-boost converter. At the start when battery is discharging the current increases and while charging the current keeps on decreases at all three variable points of time.

Third figure shows the voltage output of the boost converter which is controlled by PI controller to give stable 350V output.

3.4.1 Simulation Results of Battery Output with Change in Irradiation

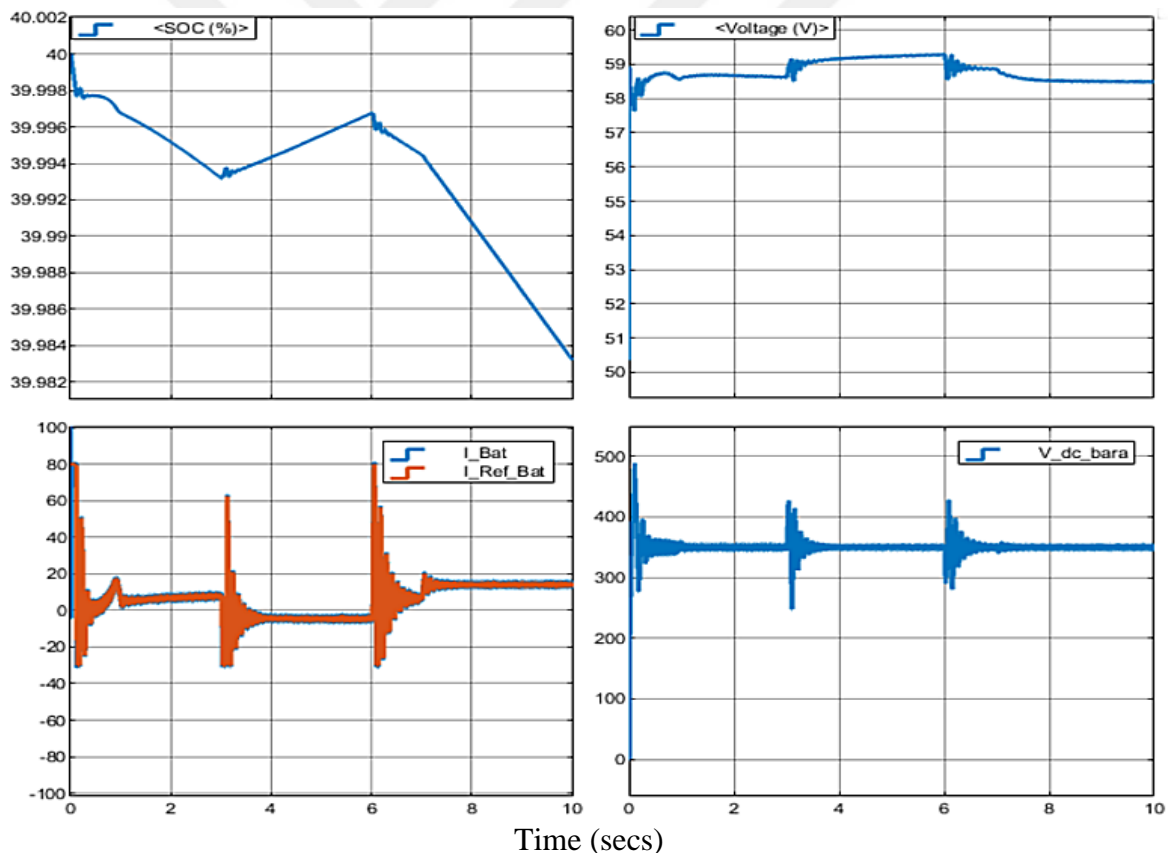


Figure 44. Battery output (a) Charging and discharging mode (b) Battery voltage (c) Battery current (d) Battery voltage

Again, in the above there figures the combination of four different result outputs of the system are given. In the first figure the result of the state of charge (SOC) of the battery is

given. From the time period of zero to 3sec battery shows continuous discharging at the $1000W/m^2$ and when the speed goes down to 1000Rpm and the irradiance also decreases from 1000 to $800W/m^2$ the battery starts charging till 6sec, again from 6sec to 10sec battery starts discharging with the increase in speed to 1300Rpm and decrease in irradiance to $500W/m^2$.

In the second figure at the right battery voltage has a little increment from zero to 3sec and then starts increasing at 1600Rpm and $1000W/m^2$. After that from 3sec to 7sec voltage starts increasing at 1000Rpm and $800W/m^2$. From 7sec to 10 sec again it starts decreasing at $500W/m^2$.

In the third figure from the left down battery current is shown with the reference value of the controlled battery current via PI controller which keeps on following the output battery current of the buck-boost converter. At the start when battery is discharging the current increases and while charging the current keeps on decreasing from 3sec to 7sec and again at the irradiance of $500W/m^2$ current starts increasing.

Third figure shows the voltage output of the boost converter which is controlled by PI controller to give stable 350V output.

3.5. Simulation Results of SPIM at Variable Speed Input

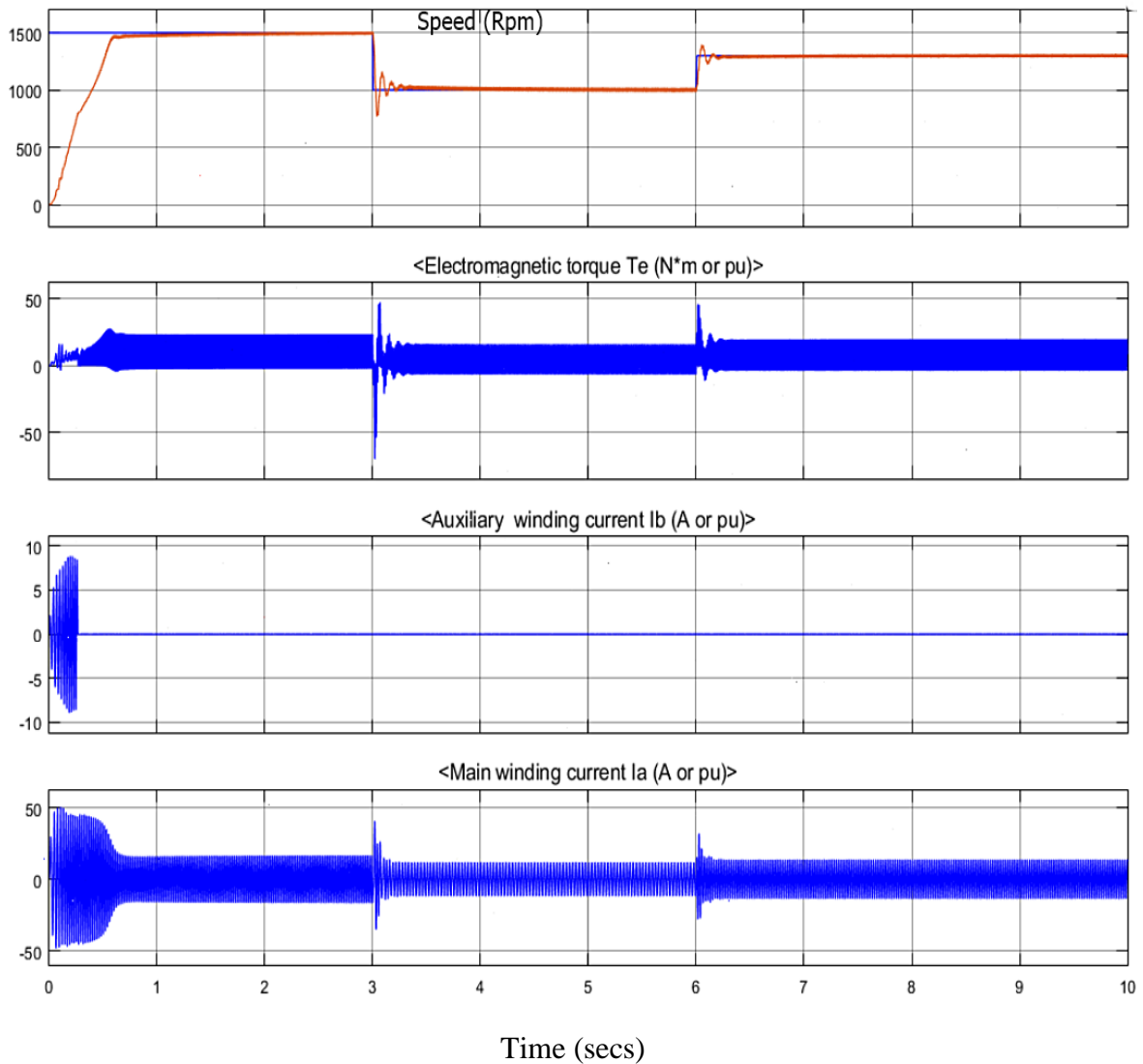


Figure 45. SPIM simulation output (a) Motor speed (b) Torque (c) Auxiliary winding current (d) Main winding current

In the above figure the speed of SPIM changes from 1600Rpm to 1000Rpm and then at the end from 1000Rpm to 1300Rpm at 3sec and 6sec.

3.6. Simulation Results of SPIM at Variable Irradiance Input

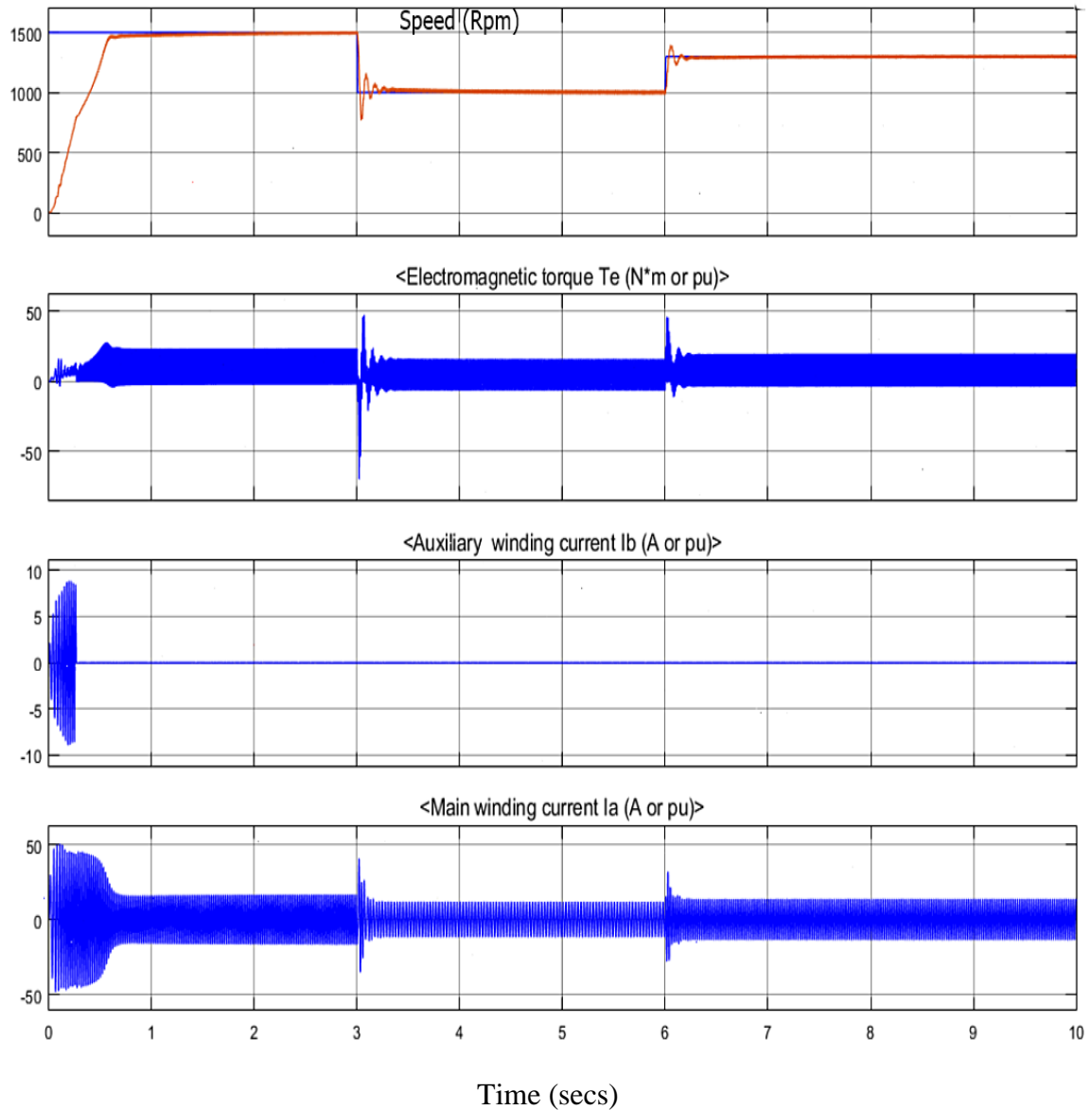


Figure 46. SPIM simulation output (a) Motor speed (b) Torque (c) Auxiliary winding current (d) Main winding current

In the above figure the speed of SPIM changes from 1600Rpm to 1000Rpm and then at the end from 1000Rpm to 1300Rpm at 3sec and 6sec at the same time period the irradiance changes from $1000W/m^2$ to $800W/m^2$ and at the end to $500W/m^2$.

3.7. Simulation Result of Speed Output of SPIM without Controller

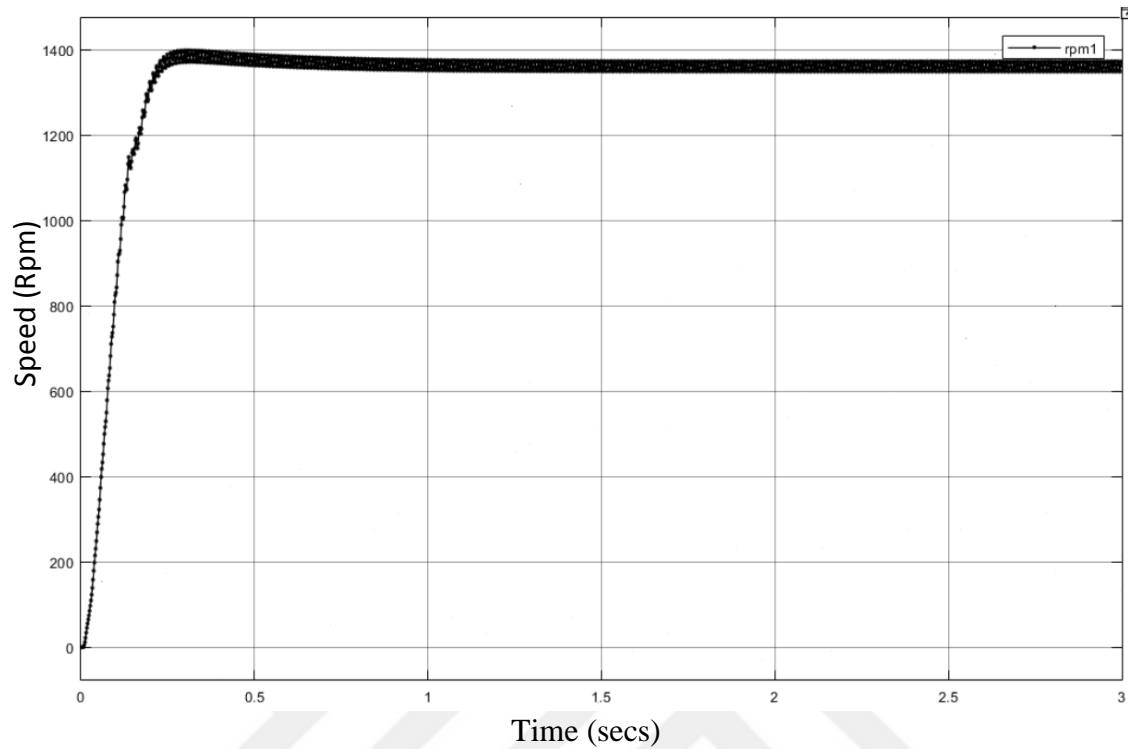


Figure 47. Speed output without controller at 1365Rpm.

3.8. Motor Main Winding Current Output

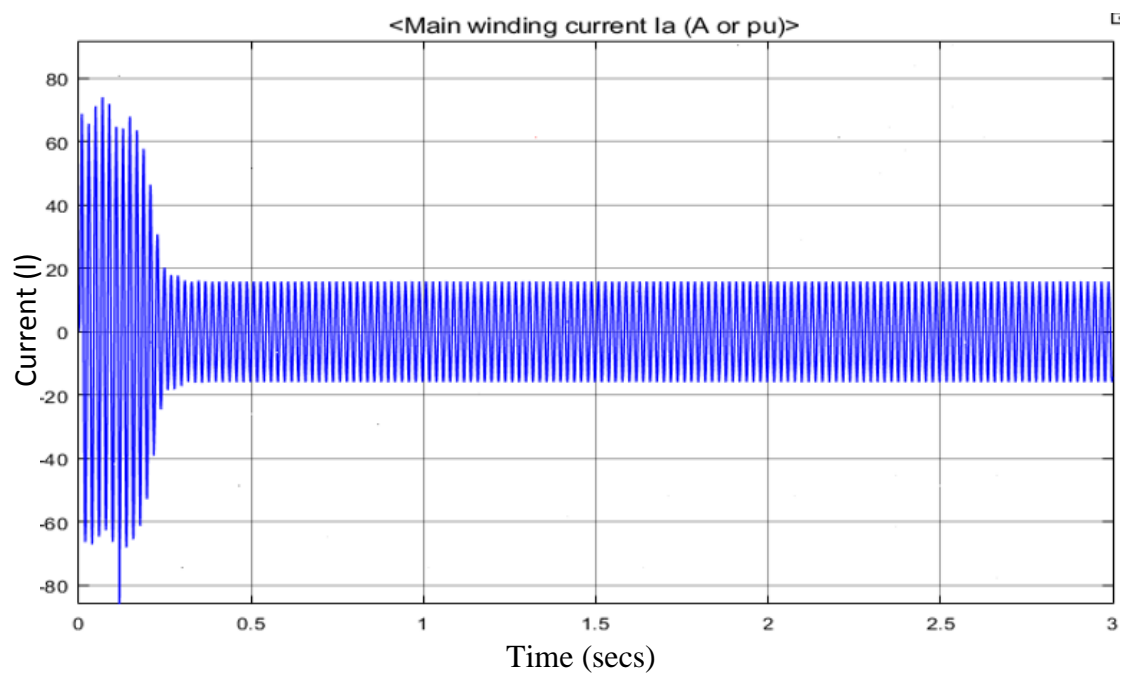


Figure 48. Main winding current (I).

4. DISCUSSION

By taking simulation results as a reference we can explain them as given below

Change of speed as input: This method is applied for the motor in order to run it or to make it useful for variable speed applications. Here in this work we are targeting the usage of this SPIM for the irrigation system of agriculture. There are several irrigation methods used for soil which depends upon the soil and weather conditions in order to supply the proper water for the crops.

Some places need the continuous water supply hourly or for a specific time frame but the amount supplying water must be well defined.

To control the supplied water, amount the most important thing is to control the motor speed in order to maintain the equilibrium.

Therefore different speed inputs are tested to control the motor for any input with the less possible time and high accuracy but there is also the disadvantage of continuous speed change as it can affect the system controller stability or some controllers are not enough for sudden speed change behavior which can harm the crops for excessive or less supply of water.

Constant speed input: The constant speed term is referred for the system without controller in which the DC output of the converter is directly given to inverter in order to get AC output to feed SPIM.

This system can be applied to fill the water Tank for the further usage of water later but it cannot be effective for the continuous water supply also a specific time period can't be determined for the filling of tank because changing weather conditions can make a lot of changes in solar panel efficiency by increasing or decreasing its irradiation continuously.

There is no feedback control so motor will adjust its speed by itself according to the supply voltage. Which makes system instable for more precise usages. As well as without controller the motor doesn't reach its full speed.

Change of irradiance: The system is tested with three different values of irradiance in order to observe the motor performance by the change produced in PV power. As according to the system, the power needed to operate the single-phase induction motor is 2Kw.

There will be a change in motor speed if the required amount of power is not enough. The change of irradiance is related to the climate change. Hence solar energy is directly converted to electricity therefore irradiance can affect the system performance most. Therefore, a battery backup is attached to the system in order to maintain its peak performance all the time.

While the low irradiance level the system is automatically transferred to battery connection which adjusts the power and voltage at the required level by using buck-boost converter and MPPT controller.

While having the maximum irradiance level at $1000W/m^2$ the battery is in charging mode for the backup. As the irradiance goes down the battery starts discharging.

There are also some important parameters needed to be study and analyze well like selecting the battery with the best backup time in order to run the motor if needed, for that purpose battery charging and discharging time must be well calculated.

MPPT controller must be designed well in order to give the precise duty cycle to find the best operating point of I-V curve to extract maximum power from the PV array at any irradiance level.

5. CONCLUSION AND FUTURE SCOPE

The main conclusion of the presented work is given here in this section. The desired work deals with the photovoltaic (PV) fed induction motor water pump system. In this entire system we have taken the single-phase induction motor drive (IMD) fed by the voltage source inverter to run and analyses the centrifugal water pump performance by providing the DC source through the DC boost converter.

The MATLAB simulation platform is used for the all analyses and performances. It is observed that the performance of the IMD is very better with the closed loop scalar control system and the v/f control system. This work has showed that the single-phase induction motor has a better performance to run the water pump as compare to three phase induction motor as we know that single phase IMD doesn't need the self-start process system. The scalar control system made the control process easy and simple which reduces the system loss and complexity. Due to the low starting torque characteristic of single-phase IMD it reaches the control level faster as compare to other motors.

Future scope

The future usage of this work is as following;

Hardware experimental results can justify the simulation results 2 the grid connected system may replace the standalone system.

MPPT and some other configurations can replace the PI controller in DC-DC converter system to get better output results. Other different control technique can be applied just as vector control or direct torque control to obtain better outputs.

A smart system can be installed for the irrigation system which can be controlled by automation intelligence to determine the humidity, temperature, motor speed, irradiance level, amount of water to deliver or to fill the water tank and many more according to requirement.

6. REFERENCES

1. Liu, B., Su, M., Yang, J., Song, D., He, D., and Song, S., Combined reactive power injection modulation and grid current distortion improvement approach for H6 transformer-less photovoltaic inverter, IEEE Transactions on Energy Conversion, 32 (2017) 1456-1467.
2. Satpathy, S., Photovoltaic power control using MPPT and boost converter. PhD diss., 2012.
3. Tang, Y., Yao, W., Loh, P. C., and Blaabjerg, F., Highly reliable transformerless photovoltaic inverters with leakage current and pulsating power elimination, IEEE Transactions on Industrial Electronics, 63 (2015) 1016-1026.
4. Jain, S., Thopukara, A. K., Karampuri, R., and Somasekhar, V. T., A single-stage photovoltaic system for a dual-inverter-fed open-end winding induction motor drive for pumping applications, IEEE Transactions on power Electronics, 30 (2014) 4809-4818.
5. Kumar, K. K., Bhaskar, R., and Koti, H., Implementation of MPPT algorithm for solar photovoltaic cell by comparing short-circuit method and incremental conductance method. Procedia Technology, 12 (2014) 705-715.
6. Scheer, H., The solar economy: Renewable energy for a sustainable global future. Routledge, 2013.
7. Kumar, R., and Singh, B., Solar PV powered BLDC motor drive for water pumping using Cuk converter, IET Electric Power Applications, 11 (2017) 222-232.
8. Lindholm, F. A., Fossum, J. G., and Burgess, E. L., Application of the superposition principle to solar-cell analysis, IEEE transactions on electron devices, 26 (1979) 165-171.
9. Harjai, A., Bhardwaj, A., and Sandhibigraha, M., Study of maximum power point tracking (MPPT) techniques in a solar photovoltaic array, PhD diss., 2011.
10. Chao, K. H., Tseng, C., Huang, H., and Liu, G., Design and implementation of a bidirectional dc-dc converter for stand-alone photovoltaic systems, International Journal of Computer, Consumer and Control, 3 (2013).
11. Edelmoser, K. H., and Himmelstoss, F. A., Bidirectional dc-to-dc converter for solar battery backup applications, IEEE 35th Annual Power Electronics Specialists Conference, June 2004, Aachen Germany, 2070-2074.

12. Chen, Y. M., Liu, Y. C., Hung, S. C., and Cheng, C. S., Multi-input inverter for grid-connected hybrid PV/wind power system, IEEE transactions on power electronics, 22, 3 (2007) 1070-1077.
13. Koutroulis, E., and Kalaitzakis, K., Novel battery charging regulation system for photovoltaic applications, IEE Proceedings-Electric Power Applications, 151, 2 (2004) 191-197.
14. Meah, K., Ula, S., and Barrett, S., Solar photovoltaic water pumping—opportunities and challenges, Renewable and Sustainable Energy Reviews, 12, 4 (2008) 1162-1175.
15. Short, T. D., and Thompson, P., Breaking the mould: solar water pumping—the challenges and the reality, Solar Energy, 75, 1 (2003) 1-9.
16. Foster, R., and Cota, A., Solar water pumping advances and comparative economics, Energy Procedia, 2014.
17. Pullenkav, T., Blunck, M., Ghose, N., and Luehr, I. M., Solar water pumping for irrigation, Opportunities in Bihar, India, 2013.
18. Foster, R., and Hanley, C., Life cycle cost analysis for photovoltaic water pumping systems in Mexico. Proceedings of the 2nd world conference on photovoltaic energy conversion, Vienna, Austria, 1998.
19. Chandel, S., Naik, M. N., and Chandel, R., Review of solar photovoltaic water pumping system technology for irrigation and community drinking water supplies, Renewable and Sustainable Energy Reviews, 49 (2015) 1084-1099.
20. Muhammad Rashid H., Third edition, “Power electronics circuit, device and application”, Chap.6, 232 (2005) 253-256.
21. Ismail, B., Taib, S., Saad, A. M., Isa, M., and Hadzer, C. M., Development of a single phase SPWM microcontroller-based inverter, In 2006 IEEE International Power and Energy Conference, November 2006, Putra Jaya Malaysia , 437-440.
22. Pandiarajan, N., and Muthu, R., Mathematical modeling of photovoltaic module with Simulink, In 2011 1st International Conference on Electrical Energy Systems (ICEES), Jan 2011, Chennai India, 258-263.
23. Kashif I., Zainal S., Saad M. and Amir S., Parameter Extraction of Solar Photovoltaic Modules Using Penalty-Based Differential Evolution, Science-Direct, 99, (2012) 297-308.
24. Mahjoubi A., Mechlouch RF., and Ben Brahim A., Data acquisition system for photovoltaic water pumping system in the desert of Tunisia, Procedia Eng. 2012.
25. Muhammad, Rashid, H., Power Electronics, Circuits, Devices, and Applications, Third Edition, Pearson Education, Inc, 2004.

26. Wong, Y., and Sumathy, K., Solar thermal water pumping systems: a review, Renew Sustain Energy Rev, 3, (1999) 185–217.
27. Komurcugil, H., Rotating-sliding-line-based sliding-mode control for single-phase UPS inverters, IEEE Transactions on Industrial Electronics, 59, 10 (2012).
28. Jeevan, K., and Soumitra, K., Study of single-phase voltage source inverter with SPWM and PWM techniques, International Journal of Current Engineering and Scientific Research (IJCESR), 5, 2 (2018).
29. Namboodiri, A., and Wani, H. S., Unipolar and bipolar PWM inverter. International Journal for Innovative Research in Science & Technology, 1,7 (2014) 237-243.
30. Liu, C., Wu, B., and Cheung, R., Advanced algorithm for MPPT control of photovoltaic systems. In Canadian Solar Buildings Conference, August 2004, Montreal Canada, 20-24.
31. Suganya, J. and Mabel, M.C., Maximum Power Point Tracker for a Photovoltaic System, International Conference on Computing, Electronics and Electrical Technologies (ICCEET '12), March 2012, Tamil Nadu India, 463–465.
32. Rashid, H., Power electronics handbook, Butterworth-Heinemann, 2017.
33. Singh, M. D., Power electronics, Tata McGraw-Hill Education, 2008.
34. Yazdani, A., and Reza, I., Voltage-sourced converters in power systems, 34. Hoboken, NJ, USA: John Wiley & Sons, 2010.
35. Xiao, H., and Xie, S., Leakage current analytical model and application in single-phase transformerless photovoltaic grid-connected inverter, IEEE Transactions on Electromagnetic Compatibility, 52, 4 (2010) 902-913.
36. Bo, L., Guo-Chun, X., and Xuan-Lü, W., Comparison of performance between bipolar and unipolar double-frequency sinusoidal pulse width modulation in a digitally controlled H-bridge inverter system, Chinese physics B, 22, 6 (2013) 060509.
37. Namboodiri, A., and Wani, H. S., Unipolar and bipolar PWM inverter. International Journal for Innovative Research in Science & Technology, 1, 7 (2014) 237-243.
38. Jidin, A., Lazi, J. M., Abdullah, A. R., Patkar, F., Kadir, A. F. A., and Hanafiah, M. M., Speed Drive Based on Torque-Slip Characteristic of the Single-Phase Induction Motor, International Conference on Power Electronics and Drives Systems, Dec 2005, Kualalumpur Malaysia, 771-775.
39. Sultani, J. F., Modelling Design and Implementation of DQ Control in Single-Phase Grid-Connected Inverters for Photovoltaic Systems used in Domestic Dwellings, 2013.
40. Fan, H., Design tips for an efficient non-inverting buck-boost converter, Analog Applications Journal, Texas Instruments, (2014) 20-25.

41. Koutroulis, E., and Kalaitzakis, K., Novel battery charging regulation system for photovoltaic applications, IEEE Proceedings-Electric Power Applications, 151, 2 (2004) 191-197.
42. Singh, B., and Kumar, R., Solar photovoltaic array fed water pump driven by brushless DC motor using Landsman converter. IET Renewable Power Generation, 10, 4 (2016) 474-484.
43. Kumar, R., and Singh, B., Solar photovoltaic array fed Luo converter-based BLDC motor driven water pumping system, 9th International Conference on Industrial and Information Systems, Dec 2014, MP India, 232-240.
44. Rocha, R., Martins Filho, L.S., and Melo, J.C.D., A speed control for variable-speed single-phase induction motor drives, Int. Symp. Industrial Electronics, Dubrovnik, Croatia, June 2005.
45. Narayana, V., Mishra, A. K., and Singh, B., Development of low-cost PV array-fed SRM drive-based water pumping system utilizing CSC converter, IET Power Electronics, 10, 2 (2017) 156-168.

CURRICULUM VITAE

I, Syed Faizan Ali Bukhari, was born in 1989 in Muzaffarabad Azad Kashmir Pakistan. Completed my secondary and high school education at Oriental Science College. Received Bachelor of Science degree in Electronics engineering from Dawood Engineering University Pakistan Karachi. Ranked Third among the 2012 graduate students. At 2015 enrolled for master's degree in Karadeniz Technical University Electrical-Electronics Engineering Department. Speak fluent English, Urdu, Punjabi, Hindi, Turkish, Polish.

